

SC-RR-70-433

AN ANALYSIS OF
THIN-WIRE CIRCULAR LOOP ANTENNAS OF ARBITRARY SIZE

L. D. Licking
D. E. Merewether
Electromagnetic Hazards Division 2627
Sandia Laboratories, Albuquerque

August 1970

ABSTRACT

A comprehensive treatment of the receiving and transmitting properties of the thin-wire circular loop antenna is provided. The response of the loop to both cw and transient excitation is considered.

The development of the theory is given, numerical data and examples are provided, and listings of the applicable FORTRAN programs are appended.



TABLE OF CONTENTS

| | <u>Page</u> |
|---|-------------|
| I. Introduction | 5 |
| II. Derivation of the Integral Equation for the Transmitting Current Distribution | 6 |
| III. Solution of the Integral Equation Using Fourier Series | 9 |
| IV. Radiated Far Field | 13 |
| V. Loop Response Due to an Incident Plane Wave | 17 |
| VI. Discussion of Results | 23 |
| A. Current Distribution | 23 |
| B. Transient Radiated Far Field | 25 |
| C. Electric Field Patterns | 27 |
| D. Receiving Transients | 27 |
| VII. Conclusions | 31 |
| References | 32 |
| APPENDIX A -- Results | 33 |
| APPENDIX B -- Computer Programs | 55 |

LIST OF ILLUSTRATIONS

| <u>Figure</u> | | <u>Page</u> |
|---------------|---|-------------|
| 1. | Geometry of the Loop | 6 |
| 2. | The Imaginary Part of the Transmitting Current Distribution on a Loop | 12 |
| 3. | Antenna Coordinate System | 14 |
| 4. | Small Loop Model | 20 |
| 5. | Open-Circuit Voltage Transfer Function | 21 |
| 6. | Short-Circuit Current Transfer Function | 21 |
| 7. | Transient Current Distribution on a Loop. $\Omega = 10$, $b = 1$ Meter | 24 |
| 8. | Transient Radiated Far Electric Field for a Loop Driven by a Step Voltage $v(t) = u(t)$ | 26 |
| 9. | Transient Radiated Far Electric Field for a Loop Driven by a Step Voltage $v(t) = u(t)$ | 26 |
| 10. | Short-Circuit Current in a Loop When Illuminated by a Unit-Step Plane Wave with $\hat{E}_o = (0, 1, 0)$ and $\hat{N} = (1, 0, 0)$ | 28 |
| 11. | Shape of the Transient Open-Circuit Voltage Waveform | 30 |

AN ANALYSIS OF THIN-WIRE CIRCULAR LOOP ANTENNAS OF ARBITRARY SIZE

I. Introduction

The purpose of this paper is to present an analysis of the transient and cw transmitting and receiving properties of loop antennas. Although loop antenna theory dates back at least to 1897, size restrictions have always limited the application of the theories. Hallen¹ and Storer² used a Fourier series solution which, according to an approximation made by Hallen, diverged after only a finite number of terms were used. Direct computation of the Fourier coefficients showed that the series did not diverge at the point predicted by Hallen. (Hallen and Storer could not calculate such a large number of coefficients because today's high-speed computers were not available to them.) In this report, a Fourier series solution is applied to loops of any circumference, provided the thin-wire approximation is satisfied.

The computer programs that were used to solve the equations are listed in Appendix B. Graphs of the results are shown in Appendix A. The graphs show:

1. Transient open-circuit voltage and short-circuit current of a loop when illuminated by a unit-step plane wave electric field.
2. Transient voltages across a load resistor when illuminated by a unit-step plane wave electric field.
3. The distant transient electric field radiated by a loop when driven by a voltage pulse.
4. The transient current on a loop when driven by a voltage pulse.
5. Field patterns of a loop when driven by the voltage $v(t) = Ve^{j\omega t}$.
6. The effect of Ω , a shape factor, on the open-circuit voltage and short-circuit current transfer functions.
7. The effect of Ω on the transient open-circuit voltage and short-circuit current.

The necessary equations are developed in Section II.

II. Derivation of the Integral Equation for the Transmitting Current Distribution³

Both the transmitting and receiving properties of the loop can be calculated from the transmitting current distribution $I_t(\phi, \omega)$.

Figure 1 shows the geometry of the problem. The loop is located in the x-y plane and is driven at $\phi = 0$ by a voltage $V e^{+j\omega t}$ applied across a thin terminal separation such that the electric field on the loop surface is $e_\phi = \frac{-V}{b} e^{+j\omega t} \delta(\phi)$. Here $\delta(\phi)$ is the Dirac delta function and b is the loop radius.

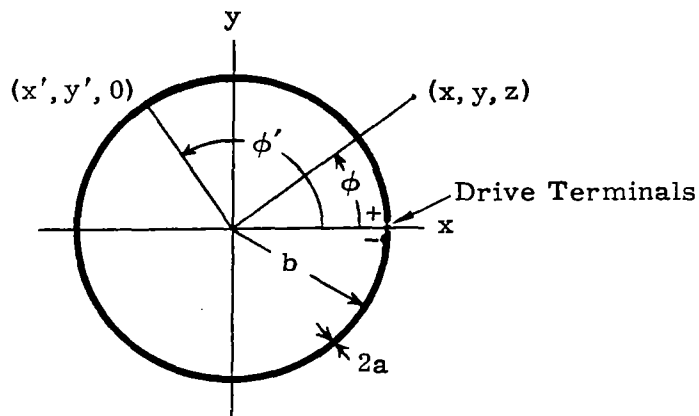


Figure 1. Geometry of the Loop

The electric field $\bar{e}(t)$ must satisfy the equation

$$\bar{e}(t) = -\frac{\partial \bar{a}}{\partial t} - \nabla \phi \quad (1)$$

Here

$$\bar{a} = \frac{\mu_0}{4\pi} \int_{\text{antenna}} \frac{\bar{i}(t - r/c)}{r} dv \quad (2)$$

= the vector potential

$$\phi = \frac{1}{4\pi\epsilon_0} \int_{\text{antenna}} \frac{\rho(t - r/c)}{r} dv \quad (3)$$

= the scalar potential

\bar{i} = the current density on the loop

ρ = the charge density on the loop

$$r = \sqrt{(x - x')^2 + (y - y')^2 + (z - z')^2} \quad (4)$$

c = the velocity of light

It will be assumed that the thin-wire approximation is satisfied ($a^2 \ll b^2$ and $k^2 a^2 \ll 1$ where a = the wire radius, b = the loop radius, and $k = \omega/c$) and that the current on the loop has a time variation of the form $e^{j\omega t}$.

Then

$$\pi a^2 \bar{i} = I_t(\phi, \omega) e^{j\omega t} \hat{a}_\phi \quad (5)$$

where \hat{a}_ϕ is a unit vector in the ϕ direction.

It will also be assumed that the loop is made of perfectly conducting wire. Then the component of electric field tangent to the conductor surface must be zero and Equation 1 implies

$$\frac{V}{b} \delta(\phi) = \frac{1}{b} \frac{\partial \Phi}{\partial \phi} + j\omega A_\phi \quad (6)$$

in cylindrical coordinates and $\frac{\partial \Phi}{\partial \phi}$ and A_ϕ are evaluated on the conductor surface (Φ and \bar{A} are the Fourier transforms of ϕ and \bar{a}). On the conductor surface

$$r \approx b \sqrt{\left(\frac{a}{b}\right)^2 + 2(1 - \cos(\phi - \phi'))}, \quad (7)$$

$$\begin{aligned} \bar{A} &= \frac{\mu_0}{4\pi} \int_{-\pi}^{\pi} \frac{I_t(\phi') e^{-jkbR(\phi-\phi')}}{bR(\phi-\phi')} \hat{a}_{\phi'} (bd\phi') \\ &= \frac{\mu_0}{4\pi} \int_{-\pi}^{\pi} \frac{I_t(\phi') e^{-jkbR(\phi-\phi')}}{R(\phi-\phi')} \left\{ \sin(\phi-\phi') \hat{a}_r + \cos(\phi-\phi') \hat{a}_\phi \right\} d\phi', \end{aligned} \quad (8)$$

$$\begin{aligned}
\Phi &= \frac{1}{4\pi\epsilon_0} \int_{-\pi}^{\pi} \left(\frac{-1}{j\omega b} \frac{\partial I_t(\phi')}{\partial \phi'} \right) \frac{e^{-jkbR(\phi-\phi')}}{bR(\phi-\phi')} (bd\phi') \\
&= \frac{-1}{4\pi\epsilon_0 j\omega b} \int_{-\pi}^{\pi} \frac{e^{-jkbR(\phi-\phi')}}{R(\phi-\phi')} \frac{\partial I_t(\phi')}{\partial \phi'} d\phi'. \tag{9}
\end{aligned}$$

Here

$$R(\phi) = \sqrt{\left(\frac{a}{b}\right)^2 + 2(1 - \cos \phi)}. \tag{10}$$

The continuity equation

$$j\omega\rho + \frac{1}{b} \frac{\partial}{\partial \phi'} \left[\frac{I_t(\phi')}{\pi a^2} \right] = 0 \tag{11}$$

was used in Equation 9 and the time variation $e^{j\omega t}$ was dropped in all equations after Equation 5. Integration of Equation 9 by parts yields

$$\Phi = \frac{j}{4\pi\epsilon_0 \omega b} \left[I_t(\phi') \frac{e^{-jkbR(\phi-\phi')}}{R(\phi-\phi')} \Big|_{\phi'=-\pi}^{\phi'=\pi} - \int_{-\pi}^{\pi} I_t(\phi') \frac{\partial}{\partial \phi'} \frac{e^{-jkbR(\phi-\phi')}}{R(\phi-\phi')} d\phi' \right] \tag{12}$$

Because $I_t(-\pi) = I_t(\pi)$, the first term in Equation 12 is zero. Since

$$\frac{\partial}{\partial \phi'} \left[\frac{e^{-jkbR(\phi-\phi')}}{R(\phi-\phi')} \right] = - \frac{\partial}{\partial \phi} \left[\frac{e^{-jkbR(\phi-\phi')}}{R(\phi-\phi')} \right]$$

Equation 12 can be written

$$\Phi = \frac{j}{4\pi\epsilon_0 \omega b} \frac{d}{d\phi} \int_{-\pi}^{\pi} I_t(\phi') \frac{e^{-jkbR(\phi-\phi')}}{R(\phi-\phi')} d\phi'. \tag{13}$$

Substitution of the ϕ component of Equations 8 and 13 into Equation 6 yields

$$V\delta(\phi) = \frac{jkb\zeta_o}{4\pi} \int_{-\pi}^{\pi} I_t(\phi') K(\phi, \phi') d\phi'. \quad (14)$$

Here

$$\zeta_o = \sqrt{\frac{\mu_o}{\epsilon_o}}$$

and

$$K(\phi, \phi') = \left[\cos(\phi - \phi') + \frac{1}{(kb)^2} \frac{d^2}{d\phi^2} \right] \frac{e^{-jkbR(\phi - \phi')}}{R(\phi - \phi')}. \quad (15)$$

Solution of Equation 14 for $I(\phi')$ gives the current distribution on a loop when driven by the voltage $V(t) = V e^{+j\omega t}$.

III. Solution of the Integral Equation Using Fourier Series²

In this section, Equation 14 is solved for $I(\phi')$. The technique is particularly amenable to computer processing. The bounded, periodic function $\frac{e^{-jkbR(\phi - \phi')}}{R(\phi - \phi')}$ can be expanded into a Fourier series as follows:

$$\frac{e^{-jkbR(\phi)}}{R(\phi)} = \sum_{n=-\infty}^{\infty} K_n e^{jn\phi} \quad (16)$$

where

$$\begin{aligned} K_n &= \frac{1}{2\pi} \int_{-\pi}^{\pi} \frac{e^{-jkbR(\phi)}}{R(\phi)} e^{-jn\phi} d\phi \\ &= \frac{1}{\pi} \int_0^{\pi} \frac{e^{-jkbR(\phi)}}{R(\phi)} \cos n\phi d\phi. \end{aligned} \quad (17)$$

Substitution of Equation 16 into Equation 15 gives

$$\begin{aligned}
K(\phi - \phi') &= \sum_{n=-\infty}^{\infty} K_n \left\{ \left(\frac{1}{kb} \right)^2 (jn)^2 + \cos(\phi - \phi') \right\} e^{jn(\phi - \phi')} \\
&= \sum_{n=-\infty}^{\infty} K_n \left\{ \frac{e^{j(\phi - \phi')} + e^{-j(\phi - \phi')}}{2} - \left(\frac{n}{kb} \right)^2 \right\} e^{jn(\phi - \phi')} \\
&= \sum_{n=-\infty}^{\infty} \left\{ \frac{K_{n+1} + K_{n-1}}{2} - \left(\frac{n}{kb} \right)^2 K_n \right\} e^{jn(\phi - \phi')} \\
&= \sum_{n=-\infty}^{\infty} \alpha_n e^{jn(\phi - \phi')}
\end{aligned} \tag{18}$$

where

$$\alpha_{-n} = \alpha_n = \frac{K_{n+1} + K_{n-1}}{2} - \left(\frac{n}{kb} \right)^2 K_n . \tag{19}$$

The integral Equation 14 can now be written as

$$V\delta(\phi) = \frac{jkb\zeta_0}{4\pi} \sum_{n=-\infty}^{\infty} \alpha_n \int_{-\pi}^{\pi} I_t(\phi') e^{jn(\phi - \phi')} d\phi' . \tag{20}$$

Expansion of $I(\phi')$ into a Fourier series gives

$$I_t(\phi') = \sum_{n=-\infty}^{\infty} I_n e^{jn\phi'} \tag{21}$$

$$I_n = \frac{1}{2\pi} \int_{-\pi}^{\pi} I_t(\phi') e^{-jn\phi'} d\phi' \tag{22}$$

and substitution of Equation 21 into Equation 20 gives

$$\begin{aligned}
 V\delta(\phi) &= \frac{jkb\zeta_o}{4\pi} \sum_{n=-\infty}^{\infty} \alpha_n I_n 2\pi e^{jn\phi} \\
 &= \frac{jkb\zeta_o}{2} \sum_{n=-\infty}^{\infty} \alpha_n I_n e^{jn\phi}.
 \end{aligned} \tag{23}$$

From Equation 23,

$$\begin{aligned}
 I_n &= \frac{2V}{jkb\zeta_o \alpha_n} \frac{1}{2\pi} \int_{-\pi}^{\pi} \delta(\phi) e^{-jn\phi} d\phi \\
 &= \frac{V}{jkb\zeta_o \pi \alpha_n}.
 \end{aligned} \tag{24}$$

Substitution of Equation 24 into Equation 21 yields the solution of Equation 14

$$\begin{aligned}
 I_t(\phi') &= \frac{V}{j\pi\zeta_o kb} \sum_{n=-\infty}^{\infty} \frac{e^{jn\phi'}}{\alpha_n} \\
 &= \frac{V}{j\pi\zeta_o kb} \left(\frac{1}{\alpha_o} + 2 \sum_{n=1}^{\infty} \frac{\cos n \phi'}{\alpha_n} \right) \\
 &= \frac{V}{j\pi\zeta_o kb} \sum_{n=1}^{\infty} \beta_n \cos (n - 1) \phi'.
 \end{aligned} \tag{25}$$

Here

$$\left. \begin{aligned}
 \beta_1 &= \frac{1}{\alpha_o} \\
 \beta_n &= \frac{2}{\alpha_{n-1}} \quad n = 2, 3, 4, \dots
 \end{aligned} \right\}. \tag{26}$$

The solution to Equation 14, $I_t(\phi')$, cannot converge at all points on the interval $-\pi \leq \phi' \leq \pi$ because the kernel $K(\phi, \phi')$ is bounded, the integration is over a finite interval, and the left side of Equation 14 is not bounded at $\phi = 0$. Other convergence difficulties were treated by Wu.⁴

In this paper, the divergence of Equation 25 was treated in the following manner. Figure 2 shows graphs of the imaginary part of $I_t(\phi)$, $I_m[I_t(\phi)]$, where each graph was constructed by summing the first q terms in Equation 25. Graphs for $q = 10, 25,$ and 60 are shown. In each graph $kb = 9$ (the loop is 9 wavelengths in circumference) and $\Omega = 2 \ln\left(\frac{2\pi b}{a}\right) = 10$.

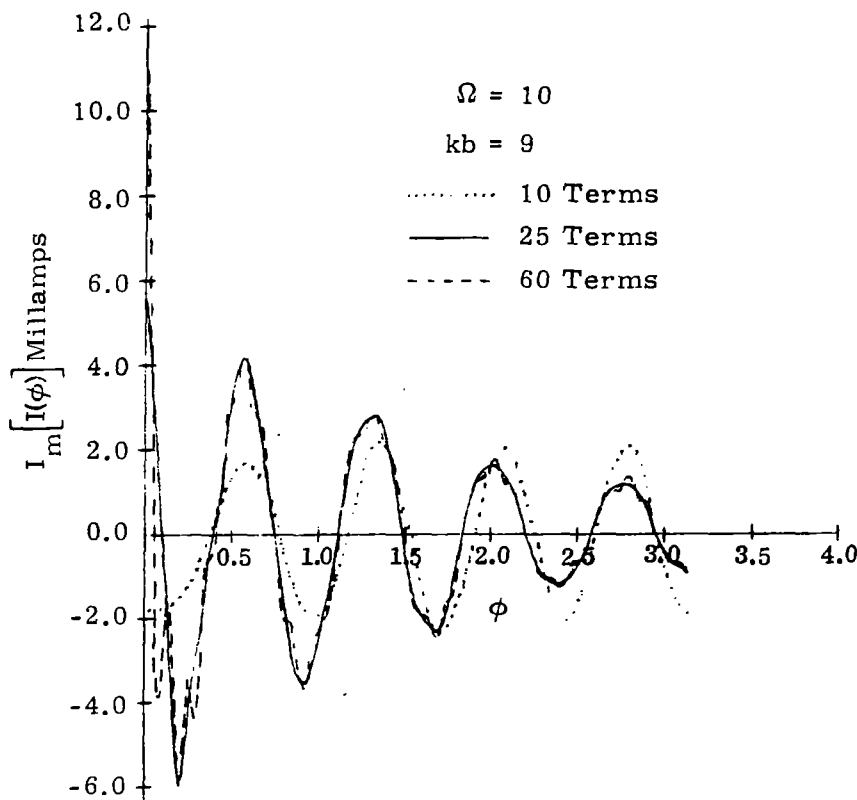


Figure 2. The Imaginary Part of the Transmitting Current Distribution on a Loop

The results show that after approximately 30 terms are used the shape of the graphs oscillates about the 30-term graph except at $\phi = 0$. At $\phi = 0$, the graph grows larger with each term added. This behavior near $\phi = 0$ results because a delta function generator $V\delta(\phi)$ was used to approximate the actual drive terminals in the mathematical model. As a consequence, too large a number of terms results in anomalous behavior in the vicinity

of the origin. For this reason, the number of terms used in the calculations in this report was limited to:

$$q = \max \{5, [3kb]\} . \quad (27)$$

Here $[3kb]$ means the largest integer n such that $n \leq 3kb$.

The real part of $I_t(\phi)$ shows much the same characteristics as the imaginary part except that it does not continue to become larger at $\phi = 0$ as the number of terms used in Equation 25 increases.

IV. Radiated Far Field

The radiated field due to a loop driven by a slice generator voltage $V e^{+j\omega t}$ can be calculated from the following equations:

$$\bar{E} = -j\omega\bar{A} - \nabla\Phi \quad (28)$$

$$\nabla \cdot \bar{A} = -j\omega\mu_0\epsilon_0\Phi \quad (29)$$

Substitution of Equation 29 into Equation 28 yields

$$\bar{E} = -j\omega\bar{A} + \frac{1}{j\omega\mu_0\epsilon_0} \nabla(\nabla \cdot \bar{A}) \quad (30)$$

It can be shown that the term $\frac{1}{j\omega\mu_0\epsilon_0} \nabla(\nabla \cdot \bar{A})$ has components with multipliers $\frac{1}{D}$, $\frac{1}{D^2}$, and $\frac{1}{D^3}$. Only the first of these has significance in the far field and it is canceled by the \hat{a}_r component of $-j\omega\bar{A}$. Thus, in the far field Equation 30 reduces to

$$\bar{E} = -j\omega(A_\theta \hat{a}_\theta + A_\phi \hat{a}_\phi) \quad (31)$$

In the above (see Figure 3)

$$D = \sqrt{(r \sin \theta \cos \phi - b \cos \phi')^2 + (r \sin \theta \sin \phi - b \sin \phi')^2 + r^2 \cos^2 \theta} \\ \approx r - b \sin \theta \cos (\phi - \phi') . \quad (32)$$

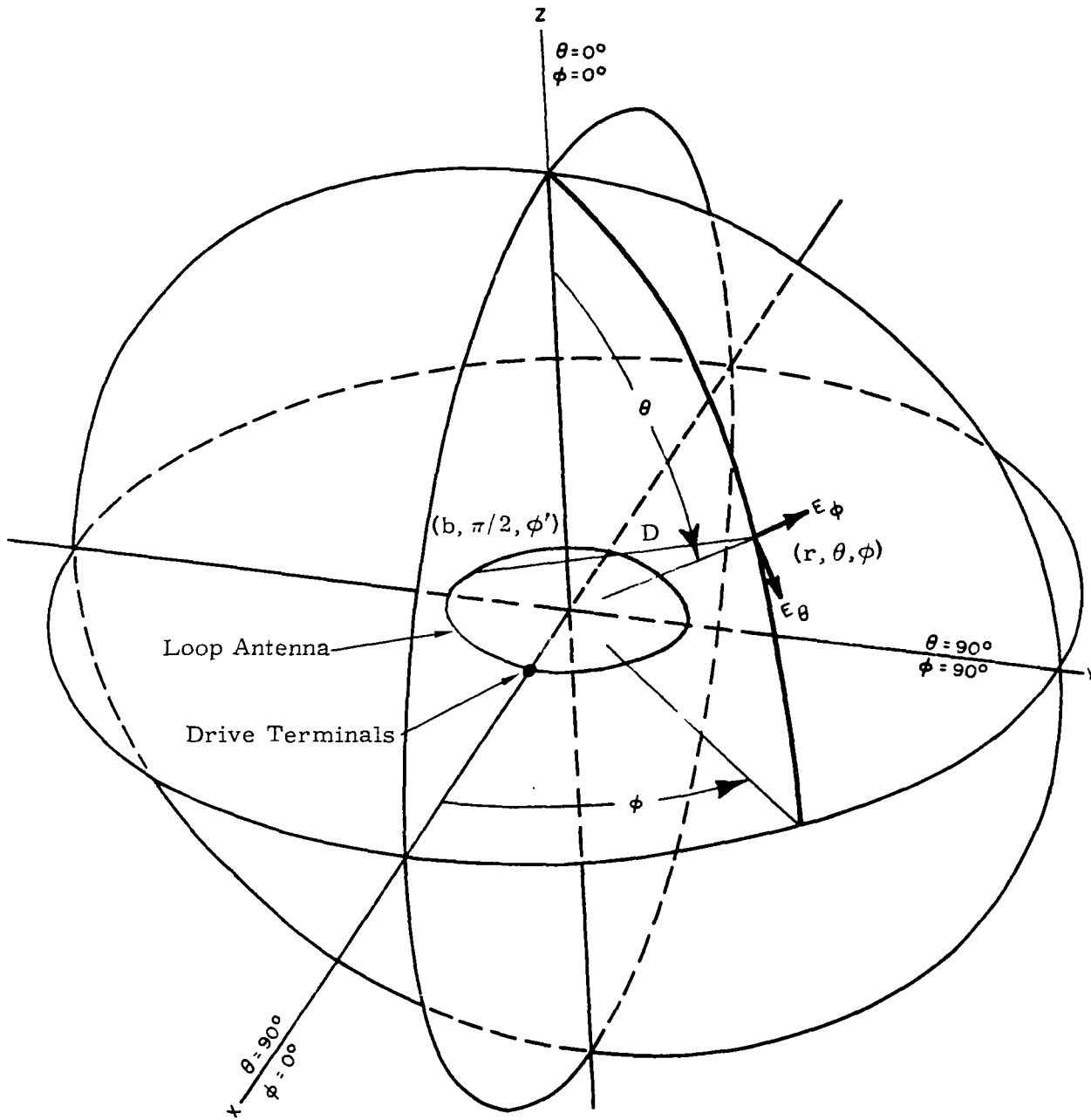


Figure 3. Antenna Coordinate System

The vector potential at the point (r, θ, ϕ) is

$$\begin{aligned} \bar{A} &= \frac{b\mu_0}{4\pi} \int_{-\pi}^{\pi} I(\phi') \hat{a}_{\phi'} \frac{e^{-jkD}}{D} d\phi' \\ &= \frac{b\mu_0}{4\pi} \int_{-\pi}^{\pi} I(\phi') \frac{e^{-jkD}}{D} \left\{ \sin \theta \sin(\phi - \phi') \hat{a}_r + \cos \theta \sin(\phi - \phi') \hat{a}_\theta + \cos(\phi - \phi') \hat{a}_\phi \right\} d\phi' \end{aligned} \quad (33)$$

In Equation 33, use of the following three equations was necessary.

$$\hat{a}_{\phi'} = -\sin \phi' \hat{a}_x + \cos \phi' \hat{a}_y \quad (34)$$

$$\hat{a}_x = \sin \theta \cos \phi \hat{a}_r + \cos \theta \cos \phi \hat{a}_\theta - \sin \phi \hat{a}_\phi \quad (35)$$

$$\hat{a}_y = \sin \theta \sin \phi \hat{a}_r + \cos \theta \sin \phi \hat{a}_\theta + \cos \phi \hat{a}_\phi \quad (36)$$

Substitution of Equations 25, 32, and 33 into Equation 31 yields

$$\begin{aligned} \bar{E} = \frac{-V}{4\pi^2 r} e^{-jkr} & \left[\cos \theta \left\{ \sum_{n=1}^q \beta_n \int_{-\pi}^{\pi} \cos\{(n-1)\phi'\} \sin(\phi - \phi') e^{jkb \sin \theta \cos(\phi - \phi')} d\phi' \right\} \hat{a}_\theta \right. \\ & \left. + \left\{ \sum_{n=1}^q \beta_n \int_{-\pi}^{\pi} \cos\{(n-1)\phi'\} \cos(\phi - \phi') e^{jkb \sin \theta \cos(\phi - \phi')} d\phi' \right\} \hat{a}_\phi \right] \quad (37) \end{aligned}$$

The approximation $D \approx r$ was used where the term $(1/D)$ appeared in the integral. Note, however, that this approximation cannot be used in e^{-jkD} .

Equation 37 yields the radiated far field solution.

An approximation for Equation 37 when $kb \ll 1$ will now be found.

By expanding $e^{jkb \sin \theta \cos(\phi - \phi')}$ into a McLaurin's series and retaining only the first two terms, the two integrals in Equation 37 become

$$\int_{-\pi}^{\pi} \cos\{(n-1)\phi'\} \sin(\phi - \phi') e^{jkb \sin \theta \cos(\phi - \phi')} d\phi' \approx \begin{cases} \pi \sin \phi & n = 2 \\ \frac{jkb\pi}{2} \sin \theta \sin 2\phi & n = 3 \\ 0 & \text{otherwise} \end{cases} \quad (38)$$

and

$$\int_{-\pi}^{\pi} \cos\{(n-1)\phi'\} \cos(\phi - \phi') e^{jkb \sin \theta \cos(\phi - \phi')} d\phi' \approx \begin{cases} jkb \pi \sin \theta & n = 1 \\ \pi \cos \phi & n = 2 \\ \frac{jkb\pi}{2} \sin \theta \cos 2\phi & n = 3 \\ 0 & \text{otherwise} \end{cases} \quad (39)$$

Equation 37 reduces to

$$\begin{aligned} \bar{E} \approx \frac{-V}{4\pi r} e^{-jkr} \left\{ \cos \theta \left[\pi \beta_2 \sin \phi + j \frac{kb\pi}{2} \beta_3 \sin \theta \sin 2\phi \right] \hat{a}_\theta \right. \\ \left. + \left[jkb \pi \sin \theta \beta_1 + \pi \beta_2 \cos \phi + j \frac{kb\pi}{2} \beta_3 \sin \theta \cos 2\phi \right] \hat{a}_\phi \right\}. \end{aligned} \quad (40)$$

From Equation 17 for $kb \ll 1$

$$K_n \approx \begin{cases} \frac{1}{\pi} \int_0^\pi \frac{d\phi}{R(\phi)} - jkb & n = 0 \\ \frac{1}{\pi} \int_0^\pi \frac{\cos n\phi d\phi}{R(\phi)} & n = 1, 2, 3, \dots \end{cases}$$

and from Equations 19 and 26

$$\begin{aligned} \beta_1 &\approx \pi \gamma_1 \\ \beta_2 &\approx -2\pi k^2 b^2 \gamma_1 \\ \beta_3 &\approx -\frac{\pi}{2} k^2 b^2 \gamma_2 \end{aligned} \quad (41)$$

Here

$$\begin{aligned} \gamma_1 &= \frac{1}{\int_0^\pi \frac{\cos \phi}{R(\phi)} d\phi} \\ \text{and} \\ \gamma_2 &= \frac{1}{\int_0^\pi \frac{\cos 2\phi}{R(\phi)} d\phi} \end{aligned} \quad (42)$$

Using Equations 41 and 42, Equation 40 can be written

$$\begin{aligned} \bar{E} &\approx \frac{Vkb}{4r} e^{-jkr} \left\{ 2kb \gamma_1 \sin \phi \cos \theta \hat{a}_\theta - \left[j \gamma_1 \sin \theta - 2kb \gamma_1 \cos \phi \right] \hat{a}_\phi \right\} \\ &\approx \frac{-jVkb\gamma_1}{4r} e^{-jkr} \sin \theta \hat{a}_\phi \end{aligned} \quad (43)$$

Equation 43 provides a simpler solution for the radiated far field under the constraint that $kb \ll 1$.

V. Loop Response Due to an Incident Plane Wave

The response of a loop to an incident plane wave electric field can be calculated from the transmitting current distribution $I_t(\phi)$ by a three-step procedure:

1. Solve for the open-circuit voltage V_{oc} of the loop when driven by the incident electric field $\bar{E}_{inc} e^{j\omega t}$ by using the equation

$$V_{oc}(\omega) = \frac{1}{I_t(0)} \int_L \bar{E}_{inc} \cdot \bar{I}_t dL. \quad (44)$$

The integration is along the length of the wire.

2. Solve for the load voltage and load current using the following equations:

$$V_L(\omega) = V_{oc}(\omega) \frac{Z_L(\omega)}{Z_A(\omega) + Z_L(\omega)} \quad (45)$$

$$I_L(\omega) = V_{oc}(\omega) \frac{1}{Z_A(\omega) + Z_L(\omega)} \quad (46)$$

$Z_A(\omega)$ = the antenna impedance

$$\begin{aligned} &= V/I_t(0) \\ &= j\pi \zeta_o kb \left(\sum_{n=1}^q \beta_n \right)^{-1} \end{aligned} \quad (47)$$

$Z_L(\omega)$ = the load impedance

3. Multiply Equations 45 and 46 by the Fourier transform of the incident electric field and take the inverse transforms of the results.

Step (1) will now be explained.

A relationship, Equation 44, between the transmitting current distribution and the open-circuit voltage is derived in Reference 5 by use of the reciprocity theorem. An incident plane wave electric field has the form

$$\bar{e}_{inc} = \hat{E}_o f\left(t - \frac{(\bar{r} - \bar{r}_o) \cdot \hat{N}}{c}\right) u\left(t - \frac{(\bar{r} - \bar{r}_o) \cdot \hat{N}}{c}\right) \quad (48)$$

with

$$\hat{\mathbf{E}}_0 \cdot \hat{\mathbf{N}} = 0. \quad (49)$$

In Equations 48 and 49, $\hat{\mathbf{N}}$ is a unit vector pointing in the direction of propagation and

$$\hat{\mathbf{N}} = l\hat{\mathbf{a}}_x + m\hat{\mathbf{a}}_y + n\hat{\mathbf{a}}_z, \quad (50)$$

$\hat{\mathbf{E}}_0$ is a constant unit vector pointing in the direction of the electric field and

$$\hat{\mathbf{E}}_0 = E_x\hat{\mathbf{a}}_x + E_y\hat{\mathbf{a}}_y + E_z\hat{\mathbf{a}}_z, \quad (51)$$

$f(t)$ is an arbitrary time function, $u(t)$ is the unit step function, c is the velocity of light,

$$\bar{\mathbf{r}} = x\hat{\mathbf{a}}_x + y\hat{\mathbf{a}}_y + z\hat{\mathbf{a}}_z, \quad (52)$$

and $\bar{\mathbf{r}}_0$ is used to define the position of the wave at $t = 0$.

Time will be defined such that $t = 0$ when the wave first contacts the loop. This definition of t requires

$$\bar{\mathbf{r}}_0 \cdot \hat{\mathbf{N}} = -b\sqrt{1 - (\hat{\mathbf{N}} \cdot \hat{\mathbf{a}}_z)^2} \quad (53)$$

The Fourier transform of Equation 48 is

$$\begin{aligned} \mathcal{F}[\bar{\mathbf{e}}_{\text{inc}}(t)] &= \hat{\mathbf{E}}_0 e^{-jkb\sqrt{1-n^2}} e^{-jk\bar{\mathbf{r}} \cdot \hat{\mathbf{N}}} F(\omega) \\ &= \bar{\mathbf{E}}_{\text{inc}} F(\omega). \end{aligned} \quad (54)$$

Here $F(\omega)$ = the Fourier transform of $f(t)$ and

$$\bar{\mathbf{E}}_{\text{inc}} = \hat{\mathbf{E}}_0 e^{-jkb\sqrt{1-n^2}} e^{-jk\bar{\mathbf{r}} \cdot \hat{\mathbf{N}}}. \quad (55)$$

Evaluation of Equation 55 at the loop and substitution of Equations 25 and 55 into Equation 44 gives

$$\begin{aligned} V_{\text{oc}}(\omega) &= b \left(\sum_{i=1}^q \beta_i \right)^{-1} e^{-jkb\sqrt{1-n^2}} \\ &\quad \left\{ \sum_{i=1}^q \beta_i \int_{-\pi}^{\pi} \cos\{(i-1)\phi\} (-E_x \sin\phi + E_y \cos\phi) e^{-jkb(l\cos\phi + m\sin\phi)} d\phi \right\}. \end{aligned} \quad (56)$$

Equation 56 is the general solution sought in Step (1).

If $kb \ll 1$, Equation 56 can be simplified in a manner similar to that used for the radiated electric field when $kb \ll 1$. For $i = 1$, the integral in Equation 56 can be written

$$\begin{aligned}
 & \int_{-\pi}^{\pi} (-E_x \sin \phi + E_y \cos \phi) e^{-jkb(l \cos \phi + m \sin \phi)} d\phi \\
 & \approx \int_{-\pi}^{\pi} (-E_x \sin \phi + E_y \cos \phi) \{1 - jkb(l \cos \phi + m \sin \phi)\} d\phi \\
 & = jkb \pi (mE_x - lE_y)
 \end{aligned} \tag{57}$$

and

$$\begin{aligned}
 V_{oc}(\omega) & \approx jk \pi b^2 (mE_x - lE_y) \\
 & = -j\omega \left[\frac{\pi b^2}{c} (lE_y - mE_x) \right].
 \end{aligned} \tag{58}$$

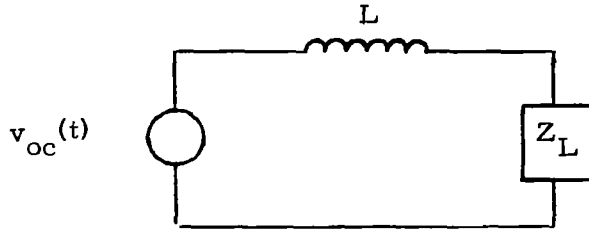
Equation 58 provides a simplified form of the solution in Equation 56 under the constraint $kb \ll 1$. These two equations complete Step (1). Step (2) is self-explanatory. In Step (3), the results of Step (2) are multiplied by $F(\omega)$, and the inverse transform is computed in order to obtain a time-domain solution. The time-domain solution of Equation 58 is

$$V_{oc}(t) = -\pi b^2 \frac{\partial b_z(t)}{\partial t} \tag{59}$$

where

$$\begin{aligned}
 b_z(t) & = \text{the } z \text{ component of the magnetic flux density} \\
 & = \frac{\hat{N} \times \hat{E}_o}{c} f(t) \Big|_{z \text{ component}} \\
 & = \frac{1}{c} (lE_y - mE_x) f(t).
 \end{aligned} \tag{60}$$

Figure 4 shows a low-frequency equivalent circuit for a loop when illuminated by a plane wave electric field.



$$v_{oc}(t) = - \frac{\partial \phi}{\partial t} = -\pi b^2 \frac{\partial b_z(t)}{\partial t}$$

ϕ is the magnetic flux linking the loop

$b_z(t)$ is the magnetic flux density

$$b_z(t) = \frac{\hat{N} \times \hat{E}_o}{c} f(t) \Big|_{z \text{ component}} = \frac{1}{c} (\ell E_y - m E_x) f(t)$$

c is the velocity of light, $c = 3 \times 10^8$ meters/sec

$$L = 1.257 \times 10^{-6} b \left[\ln\left(\frac{8b}{a}\right) - 2 \right] \text{ henries}$$

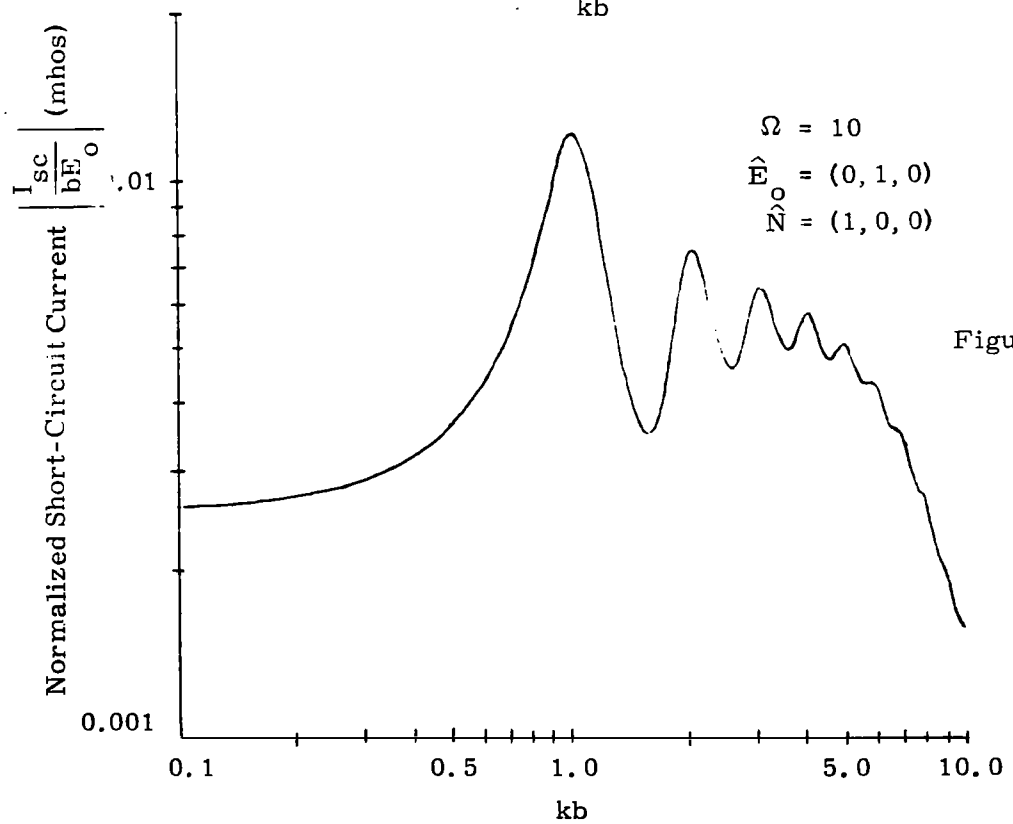
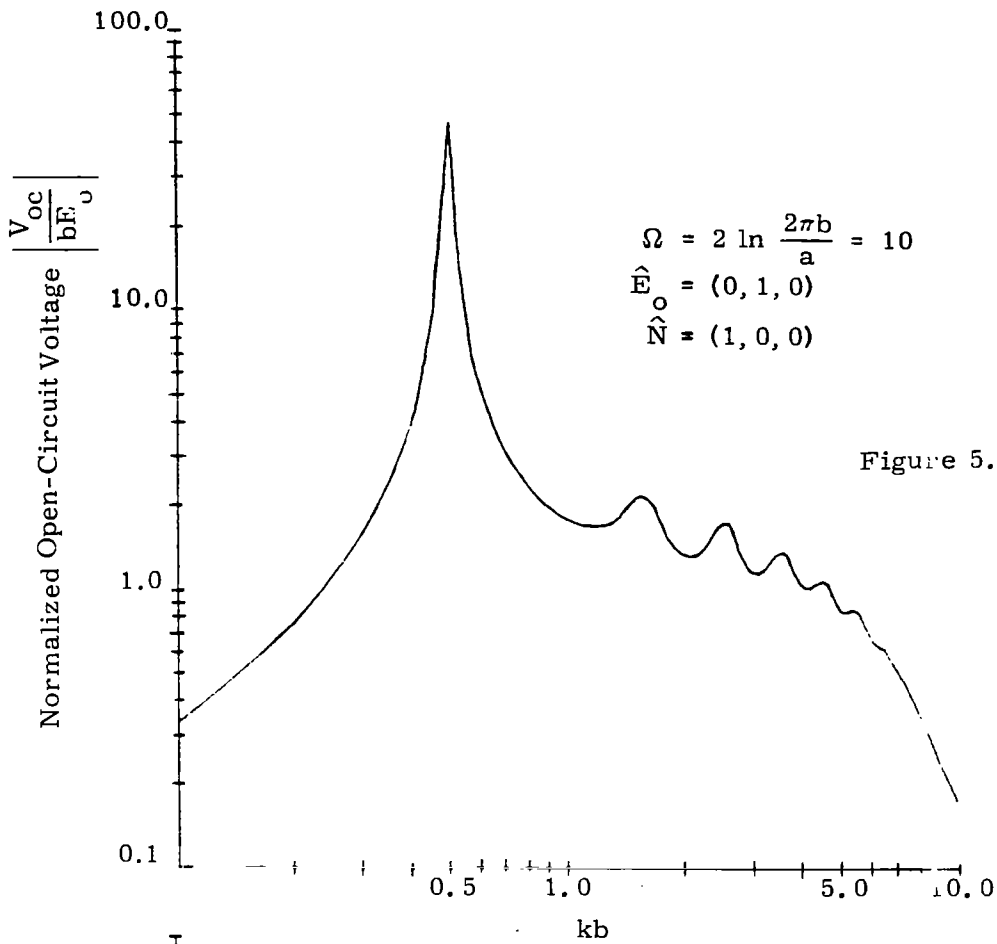
b, a are the loop and wire radii in meters

The loop is small $\left(k_o b = \frac{2\pi f b}{c} \leq 0.1 \right)$

at highest frequency of interest.

Figure 4. Small Loop Model

The magnitude of the open-circuit voltage ($V_{oc}(\omega)$ of Equation 56) is plotted versus kb in Figure 5. The plane wave is propagating in the direction of the positive x axis and the electric field is polarized in the direction of the y axis. Figure 6 is a graph of the short-circuit current ($I_L(\omega)$ of Equation 46 with $Z_L(\omega) = 0$) of the loop for the same incident plane wave electric field. These graphs show that the first and largest resonant frequency of the open-circuit voltage occurs when the circumference of the loop is one-half wavelength $\left(\frac{2\pi b}{\lambda} = kb = 1/2 \right)$ and that the resonant frequency of the short-circuit current is double that of the open-circuit voltage $\left(\frac{2\pi b}{\lambda} = kb = 1 \right)$. The loop must be a full wavelength around for a reinforcement of the current to occur.



In all cases studied, it was found that the open-circuit voltage has a resonant frequency where the circumference of the loop is one-half wavelength and in all cases but one the short-circuit current resonates where the circumference is one wavelength. It was found that when the plane wave propagates in the direction of the negative y axis the first short-circuit current resonance occurs when the circumference of the loop is two wavelengths. Since the loop terminals are shorted when the short-circuit current is calculated, the two cases mentioned above differ only in the position where the current is measured, which shows that the resonant frequency of the short-circuit current on a loop can vary with position on the loop. These results are discussed further in the following material.

Transient signals may be derived from the steady-state solutions found above by use of

$$r(t) = \frac{2}{\pi} \int_0^{\infty} \text{Re}[F(\omega) T(\omega)] \cos \omega t \, d\omega, \quad t \geq 0. \quad (61)$$

Here $r(t)$ is the transient response, $T(\omega)$ is the transfer function for the parameter of interest [$T(\omega) = R(\omega)/F(\omega)$ and $R(\omega)$ is the Fourier transform of $r(t)$], and $F(\omega)$ is the forcing function. Equation 61 is valid for all real causal functions.

All transient responses presented in this report except the transmitting current distribution were found by a direct application of Equation 61. The transient transmitting current distribution can be simplified as follows.

Substitution of Equation 25 into Equation 61 gives

$$\begin{aligned} i(t, \phi) &= \frac{2}{\pi} \int_0^{\infty} \text{Re} \left[\frac{V(\omega)}{j\pi\zeta_0 kb} \sum_{n=1}^q \beta_n \cos(n-1)\phi \right] \cos \omega t \, d\omega \\ &= \frac{2c}{\pi^2 \zeta_0 b} \sum_{n=1}^q \left\{ \int_0^{\infty} \text{Re} \left[\frac{V(\omega)}{j\omega} \beta_n \right] \cos \omega t \, d\omega \right\} \cos(n-1)\phi \\ &= \frac{2c}{\pi^2 \zeta_0 b} \sum_{n=1}^q \xi_n(t) \cos(n-1)\phi \end{aligned} \quad (62)$$

where

$$\xi_n(t) = \int_0^{\infty} \text{Re} \left[\frac{V(\omega)}{j\omega} \beta_n \right] \cos \omega t \, d\omega. \quad (63)$$

Note that the current on the loop can be evaluated at any position on the loop when the numerical values of $\xi_n(t)$ for $n = 1, 2, \dots, q$ are known at time t . In Equation 62, the position parameter ϕ can be separated from time t . Equations for the transient radiated field and the receiving load voltages and currents cannot be factored into functions of t only and position only and, therefore, the inverse transform must be computed at each position of interest.

VI. Discussion of Results

In this section, various specific results of interest are presented, along with a discussion of the salient features of the solution behavior.

A. Current Distribution

The current distribution on a loop when driven by the voltage

$$v(t) = \left\{ 1 - (1 + t/a) e^{-t/a} \right\} e^{-t} u(t) \quad (64)$$

where

$$a = 1.33 \times 10^{-9} \text{ sec}$$

(Figure 7) was calculated by using Equations 62 and 63. Equation 64 was chosen to give a fast rise time (about 6 nanoseconds) and a long fall time (0.7 second to half value). For this drive voltage $\xi_1(t)$ does not have a Fourier transform because

$$\lim_{t \rightarrow \infty} \xi_1(t) = \text{constant} \neq 0.$$

$\xi_1(t)$ was found by calculating

$$\frac{d\xi_1(t)}{dt} = \int_0^\infty \text{Re} \left[V(\omega) \beta_1 \right] \cos \omega t \, d\omega \quad (65)$$

and then numerically integrating $\frac{d\xi_1(t)}{dt}$.

Figure 7 shows that a positive current wave is launched from the loop terminals and is propagated in both directions around the loop. As the current wave propagates around the loop the slope of the leading edges is rapidly reduced.

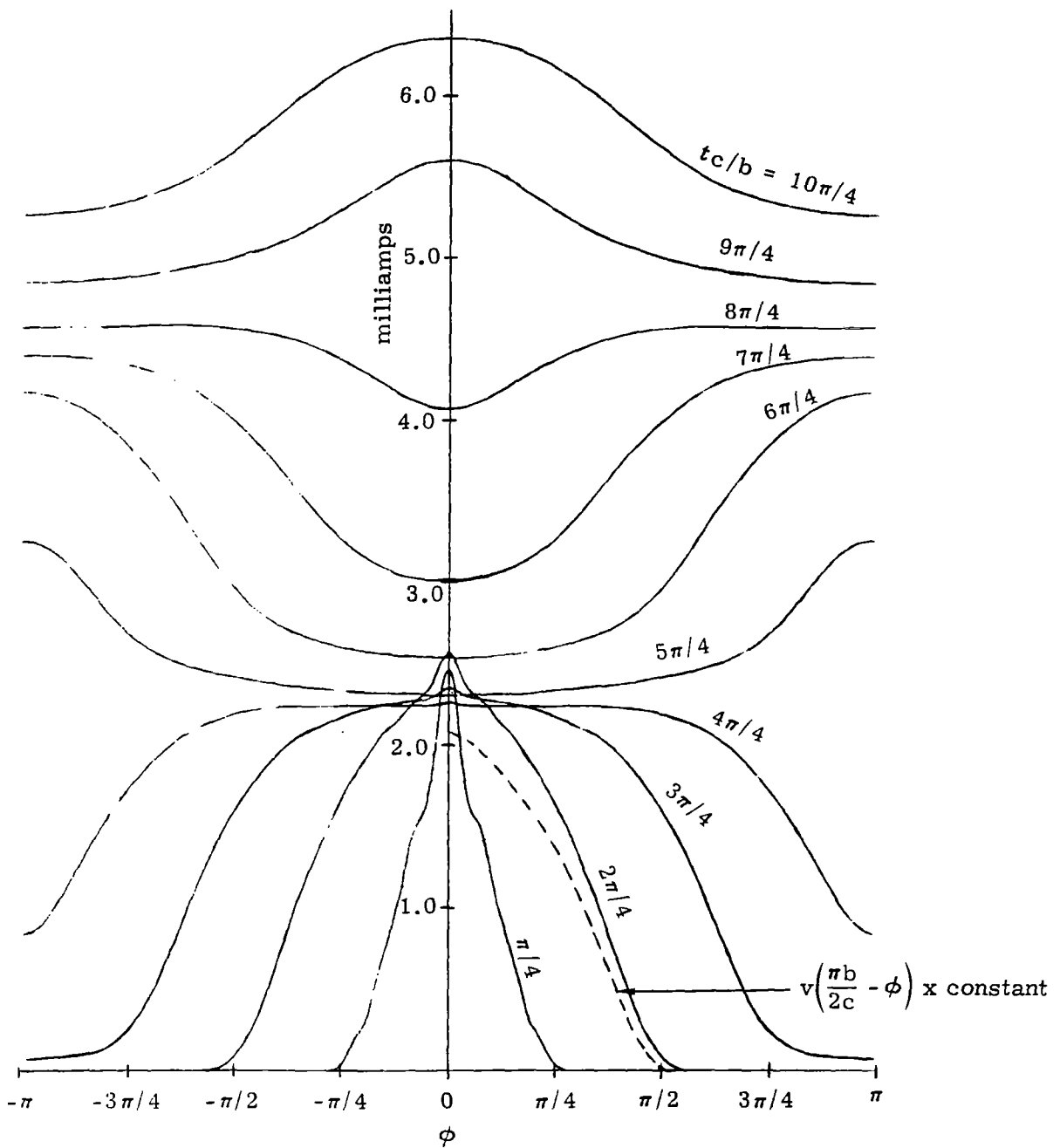


Figure 7. Transient Current Distribution on a Loop. $\Omega = 10$, $b = 1$ Meter

Also shown in Figure 7 is a plot of the transient driving voltage which is plotted as if it were propagating undistorted around the loop at the speed of light. The graph of the voltage pulse has been scaled so that the maximum value of the voltage pulse is the same height as the current curve at $tc/b = \pi$. Note that the rise time of the current is shorter than that of the drive voltage for an observer located at $0 < |\phi| < (\sim \frac{\pi}{2})$ and $tc/b < (\sim \frac{\pi}{2})$.

It is interesting to compare the value of the current in the loop to that in an inductor, with the same low-frequency inductance, when driven by a unit step. For an inductor

$$i(t) = \frac{t}{L} = \frac{1}{3.9 \times 10^{-6}} \left(\frac{10\pi}{4 \times 3 \times 10^8} \right) = 6.7 \times 10^{-3} \text{ amp}$$

at $tc/b = \frac{10\pi}{4}$. From Figure 7

$$i = 6.4 \times 10^{-3} \text{ amp}$$

at $tc/b = \frac{10\pi}{4}$. Thus the two results are quite comparable.

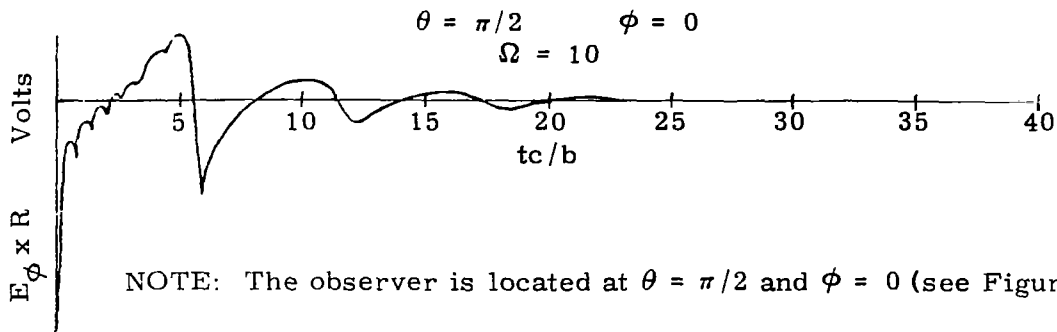
B. Transient Radiated Far Field

The high-frequency content of the driving pulse is accentuated in the transient far field as can be seen by examination of Equations 1 and 2 or 31. Equations 1 and 2 show that the electric field is proportional to the derivative of the vector sum of the current density on the loop. As noted above, the rise time of the current near $t = 0$ is faster than that of the applied voltage. This fast-rising current near $t = 0$ causes the high-frequency content of the drive voltage to be accentuated even more.

Figure 8 shows the calculated transient electric field, for an observer located at $\theta = \pi/2$ and $\phi = 0$, of a loop driven by the voltage $v(t) = u(t)$.

This voltage pulse has an infinite derivative at $t = 0$ and, as a result, the electric field has its maximum absolute value when the leading edge of the electric field pulse arrives at the observer for observers in the $\phi = 0$ plane. In Figure 8, time is retarded by the amount $\frac{r - b \sin \theta \cos \phi}{c}$ so that $t = 0$ corresponds to the time when the radiated field first arrives at the observer. Equation 2 shows that $a_\phi(t)$ has its maximum rate of change at $t = 0$. As the current pulse travels around the loop there is no change in $a_\phi(t)$, as viewed from $\phi = 0$, at the time when $tc/b = \pi/2$, that is,

$$\left. \frac{d a_\phi(t)}{dt} \right|_{\substack{\phi = 0 \\ t = \pi b/2c}} = 0.$$

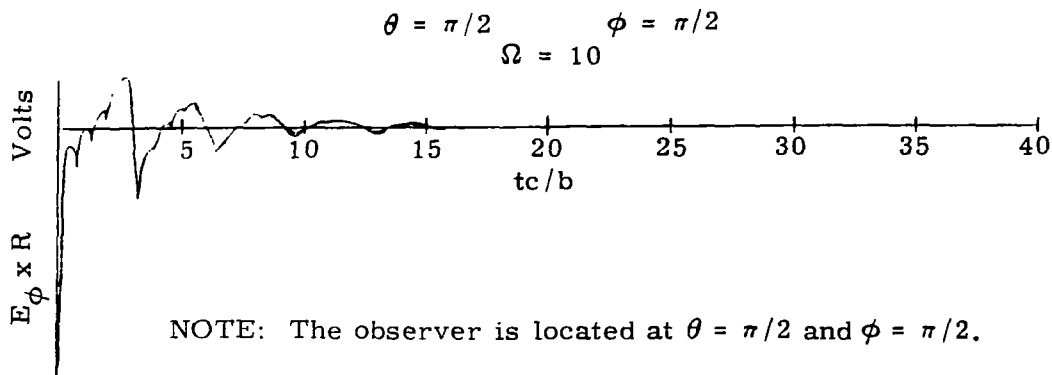


NOTE: The observer is located at $\theta = \pi/2$ and $\phi = 0$ (see Figure 3).

Figure 8. Transient Radiated Far Electric Field for a Loop Driven by a Step Voltage $v(t) = u(t)$

Time is now retarded by the additional amount b/c (the leading edge the current pulse is moving away from the observer) so that the electric field should go to zero at $tc/b = \frac{\pi}{2} + 1 \approx 2.6$ as is shown in Figure 8. As the current pulse progresses on around the loop, $a_{\phi} \Big|_{\phi=0}$ begins to have a negative derivative which reaches a local maximum (in absolute value) at $tc/b = \pi + 2$. Another zero should occur at $tc/b = \frac{3\pi}{2} + 1$ and another local maximum absolute value at $tc/b = 2\pi$. This pattern should repeat as the leading edges of the current pulse make another revolution around the loop and have a period of $tc/b = 2\pi$. All of the above features are evident in Figure 8. The rapid decrease in the slope of the leading edges of the current wave (Figure 7) causes a change in the shape and magnitude of the otherwise periodic signal.

Now, consider an observer located at $\theta = \pi/2$ and $\phi = \pi/2$. At $\phi = \pi/2$, the current wave must be considered in two parts: the wave propagating around the loop in the direction of increasing ϕ and that one propagating in the opposite direction. Separate analysis of these two current waves and addition of the results give a transient of the same shape as at $\phi = 0$ except that the frequency is doubled as shown in Figure 9.



NOTE: The observer is located at $\theta = \pi/2$ and $\phi = \pi/2$.

Figure 9. Transient Radiated Far Electric Field for a Loop Driven by a Step Voltage $v(t) = u(t)$

Transient radiated electric fields for a loop when driven by a voltage of the form given by Equation 64 are shown in Appendix A. The voltage waveform has a rise time of $5a = 6.66 \times 10^{-9}$ sec and has a zero derivative at $t = 0$. This zero derivative cuts down the high-frequency content of the radiated field and changes the appearance of the electric field for values of t near zero. The loop has a radius of 1 meter and $\Omega = 10, 12,$ and 14 . The field is evaluated at several values of θ and ϕ when $\Omega = 10$.

C. Electric Field Patterns

Field patterns in the planes $\phi = 0$, $\phi = \pi/2$, and $\theta = \pi/2$ were calculated for $kb = 1, 1.5, 2, 2.5, \dots, 10$ and for $\Omega = 10$.

In the planes $\phi = 0$ (Figure A18 of Appendix A) and $\theta = \pi/2$ (Figure A17 of Appendix A), the θ component of the electric field E_θ is zero. Therefore, these patterns are patterns of the total electric field E_t as well as of the ϕ component E_ϕ . In general

$$E_t = \sqrt{E_\theta E_\theta^* + E_\phi E_\phi^*}$$

where the asterisk denotes the complex conjugate.

The patterns of E_ϕ (Figures A19), E_θ (Figure A20), and E_t (Figure A21) were calculated in the plane $\phi = \frac{\pi}{2}$.

D. Receiving Transients

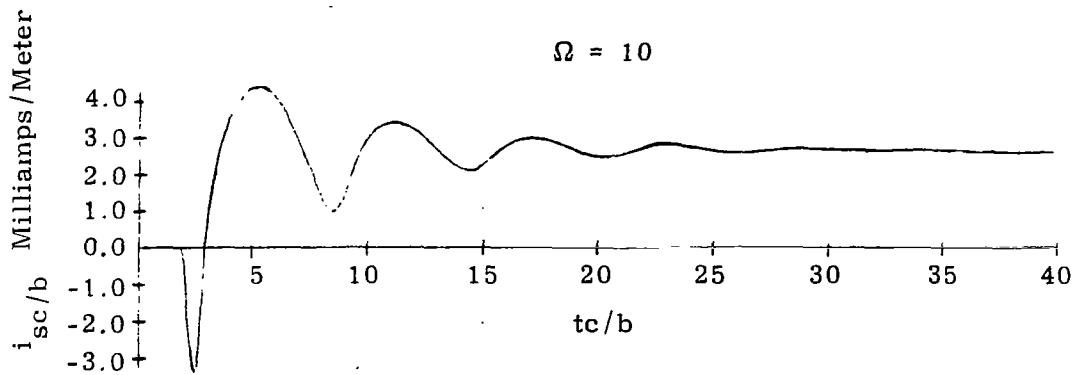
Transient load voltages and load currents were calculated from Equations 45 and 46 for a loop when illuminated by a unit-step plane wave. The frequency response of the loop falls off at the high-frequency end fast enough that the inverse integral of the Fourier transform can be truncated at $kb = 10$ with negligible effects on the results.

Transient responses are shown in Appendix A for various directions of propagation and polarization of the incident electric field. Graphs showing the effects of a load resistor and $\Omega = 2 \ln \frac{2\pi b}{a}$ are also shown.

Consider Figure 10 which shows the short-circuit current induced in a loop by a unit-step plane wave which is propagating down the x axis and the electric field is polarized in the y direction. An explanation of the shape of the transient short-circuit current follows.

Since $t = 0$ at the instant of time when the wave first contacts the loop, no signal can be seen at the terminals until $tc/b = 2$. At $tc/b = 2$, the electric field arrives at the loop

terminals and is parallel to the wire at this point. By assuming that a current wave, which is proportional to that component of the incident electric field parallel to the wire, propagates in the clockwise and counterclockwise directions from each point on the wire, it can be seen that a negative current should flow at the terminals and should reach a maximum in absolute value when $tc/b = 1 + \pi/2$. Note that $tc/b = 1 + \pi/2$ corresponds to the time when that contribution to the total current from the points $\phi = \pm\pi/2$ arrives at the terminals. At points on the loop where $\pi/2 < |\phi| < \pi$ positive current waves are launched. Maximum current contributions should arrive at the terminals at $tc/b = \frac{3\pi}{2} + 1$. Since the loop is shorted the current waves continue to propagate around the loop in their original directions. The next minimum of current should occur at $tc/b = (2\pi + \text{the first minimum}) = 1 + \pi/2 + 2\pi$. All of the above features are evident in Figure 10.



NOTE: The loop orientation is shown in Figure 1.

Figure 10. Short-Circuit Current in a Loop When Illuminated by a Unit-Step Plane Wave with $\hat{E}_0 = (0, 1, 0)$ and $\hat{N} = (1, 0, 0)$

A similar line of reasoning can be used to predict the loop response when the wave is propagating down the y axis in the negative direction and the electric field is polarized in the direction of the negative x axis. Here the analysis is more complicated than the first example and is best handled by considering each of the four quadrants of the loop separately and then adding the results. The final result in this case is a current which has a resonant frequency twice as high as the first example. This double resonant frequency is similar to the case of the radiated field at $\phi = \theta = \pi/2$. A line of reasoning to predict the open-circuit voltage waveform of a loop can also be devised. This explanation is the same as the short-circuit explanation except that the voltage waves are reflected and inverted at the open loop terminals. An example of an explanatory analysis follows.

Consider Figure 11 which shows an incident plane wave propagating down the x axis and the electric field polarized in the y direction. Since $t = 0$ at the time when the leading edge first touches the loop, no signal is seen until $tc/b = 2$. Consider quadrant 1 as marked on the diagram of Figure 11. At $tc/b = 2$, the electric field step arrives at and is parallel to the loop terminals. Effects of clockwise propagating waves from quadrant 1 will continue to accumulate at the loop terminals during the time interval from $tc/b = 2$ until $tc/b = 1 + \pi/2$. This effect is shown in the top curve of Figure 11. The voltage wave will be reflected at the open-loop terminals and will appear at a time interval $2\pi(b/c)$ later. Since the wave is inverted when it is reflected, the reflected wave will cancel the effect of the original wave for the next time interval of length $2\pi(b/c)$ as shown in the top curve of Figure 11.

The wave of quadrant 1 which propagates in the counterclockwise direction has no effect until $tc/b = 1 + \frac{3\pi}{2}$ and will continue to accumulate until $tc/b = 2 + 2\pi$ (the second curve from the top). This procedure was followed for the 2nd, 3rd, and 4th quadrants and the resulting eight curves were then added to form the result shown. For small values of tc/b , this curve looks very similar to the curve (also shown in Figure 11) which was calculated from Equations 56 and 61. For larger values of tc/b , the high frequencies necessary to form the sharp spikes of the waveform are lost because of radiation from the loop, and the resonant frequency of the open-circuit voltage is all that remains. Note that the second spike in the waveform begins to appear at $tc/b = 1 + \pi/2 + 2\pi$ for the thin loop ($\Omega = 14$). For loops with lower values of Ω the second spike cannot be seen.

The explanations given above for the various waveforms give an intuitive picture of the transient behavior exhibited in the calculated solutions. This provides a feel for what is going and also demonstrates the validity of the numerical results.

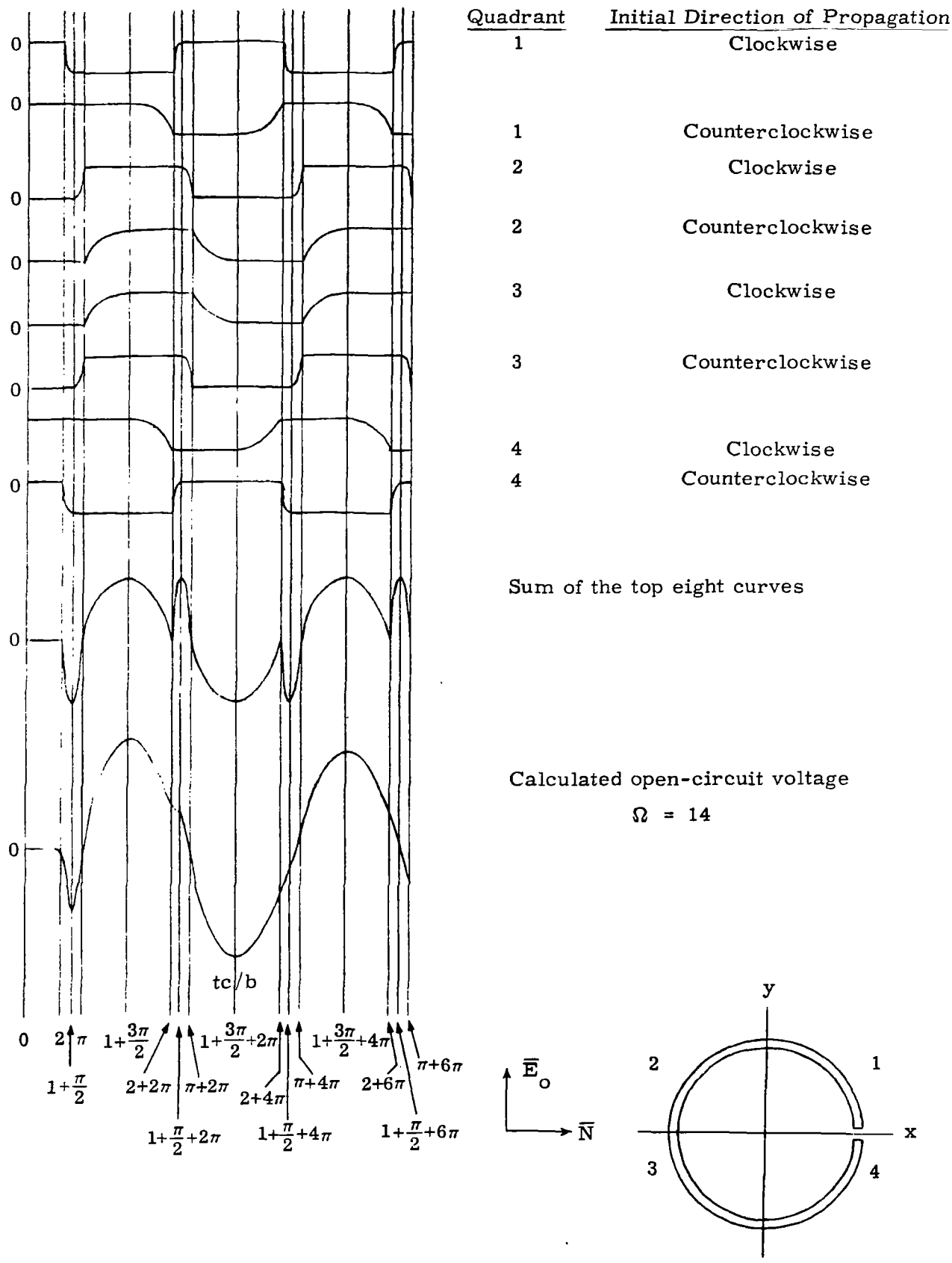


Figure 11. Shape of the Transient Open-Circuit Voltage Waveform

VII. Conclusions

The transmitting current distribution on a circular loop antenna when driven by a voltage of the form $v(t) = V_0 e^{j\omega t}$ was obtained by a Fourier series solution. Using the transmitting current distribution the following loop antenna responses were calculated.

1. The transient transmitting current distribution.
2. The transient load voltages and load currents when illuminated by a transient plane wave electromagnetic field.
3. Transient far field waveforms when driven by a transient drive voltage.
4. Field patterns when driven by the voltage $v(t) = V_0 e^{j\omega t}$.

The effects of Ω on the responses of circular loop antennas were also investigated. Here $\lambda = 2 \ln \frac{2\pi b}{a}$, b is the radius of the loop, and a is the radius of the wire which forms the loop.

It was shown that the calculated transient waveforms were in good agreement with intuitively constructed waveforms.

References

1. "Theoretical Investigations into the Transmitting and Receiving Qualities of Antennae," E. Hallen, Nora Acta Regiae Soc. Sci. Upsaliensis, Vol. 11, No. 4, November 1938.
2. "Impedance of Thin-Wire Loop Antennas," J. E. Storer, Transactions of AIEE, Vol. 75, Part 1, 1956, pp. 606-619.
3. "The Impedance Characteristics of Antennas Involving Loop and Linear Elements," Tang Chang, Technical Report No. 16, Cruft Laboratory, Harvard University, Cambridge, Massachusetts, July 1947, pp. 12-14.
4. "Theory of the Thin Circular Loop Antenna," T. T. Wu, Journal of Mathematical Physics, Vol. 3, No. 6, November - December, 1962, pp. 1301-1304.
5. Electromagnetic Theory for Engineering Applications, W. L. Weeks, John Wiley and Sons, Inc., New York, 1964, p. 333.

APPENDIX A

Results

APPENDIX A

Results

Transmitting Current Distribution

Figure A1 shows the transient transmitting current distribution on a loop when driven at $\phi = 0$ by the voltage

$$v(t) = \left\{ 1 - (1 + t/a)e^{-t/a} \right\} e^{-t} u(t)$$

The current distribution is plotted versus ϕ for the instants of time such that $tc/b = i\pi/4$, $i = 1, 2, \dots, 10$.

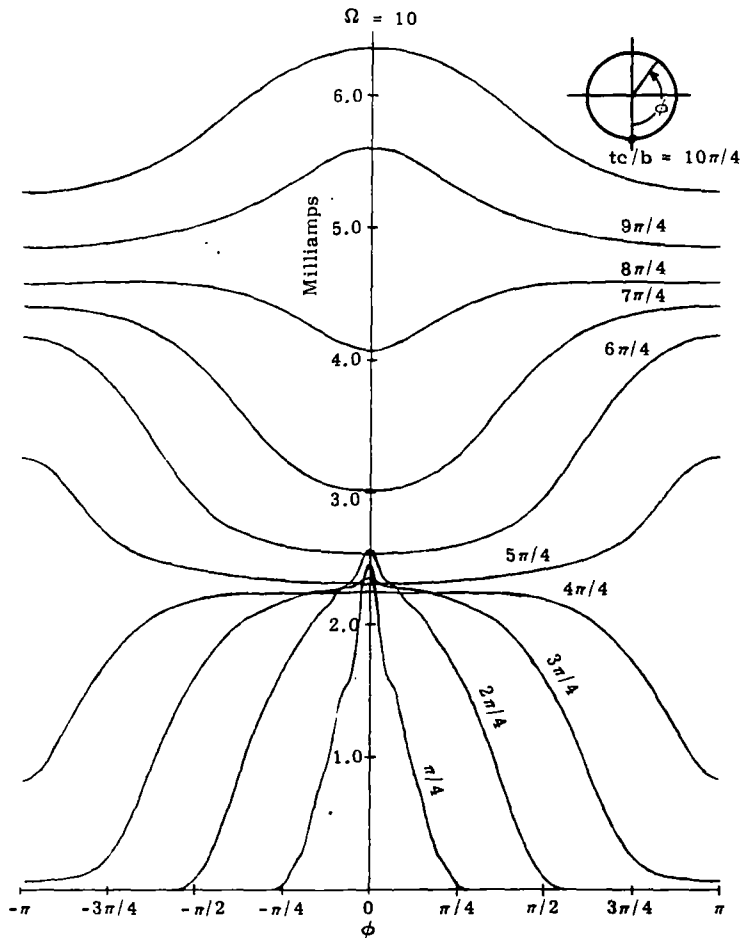


Figure A1. Transmitting Current Distribution

Effect of Ω on the Transfer Functions

Figures A2 and A3 show the effect of $\Omega = 2 \ln \frac{2\pi a}{b}$ on the open-circuit voltage and short-circuit current transfer functions for $\hat{E}_o = (0, 1, 0)$ and $\hat{N} = (1, 0, 0)$. Values of the transfer functions are normalized by the radius of the loop b . To find the actual value of the magnitude of a transfer function, multiply the value of the ordinate of interest by the radius of the loop under consideration. For example, if $b = 2$ meters and $\Omega = 14$, the value of the open-circuit voltage transfer function at $kb = 0.5$ is $72 (2 \text{ meters}) = 144$ meters.

That the indicated normalization is valid can be seen by examination of Equations 56, 45, 46, 47, 26, 19, and 17. These equations show that the load voltage or load current can be written as b times a function of kb and Ω , that is, for V_L ,

$$V_L = bT(kb, \Omega)$$

or

$$V_L/b = T(kb, \Omega)$$

(A1)

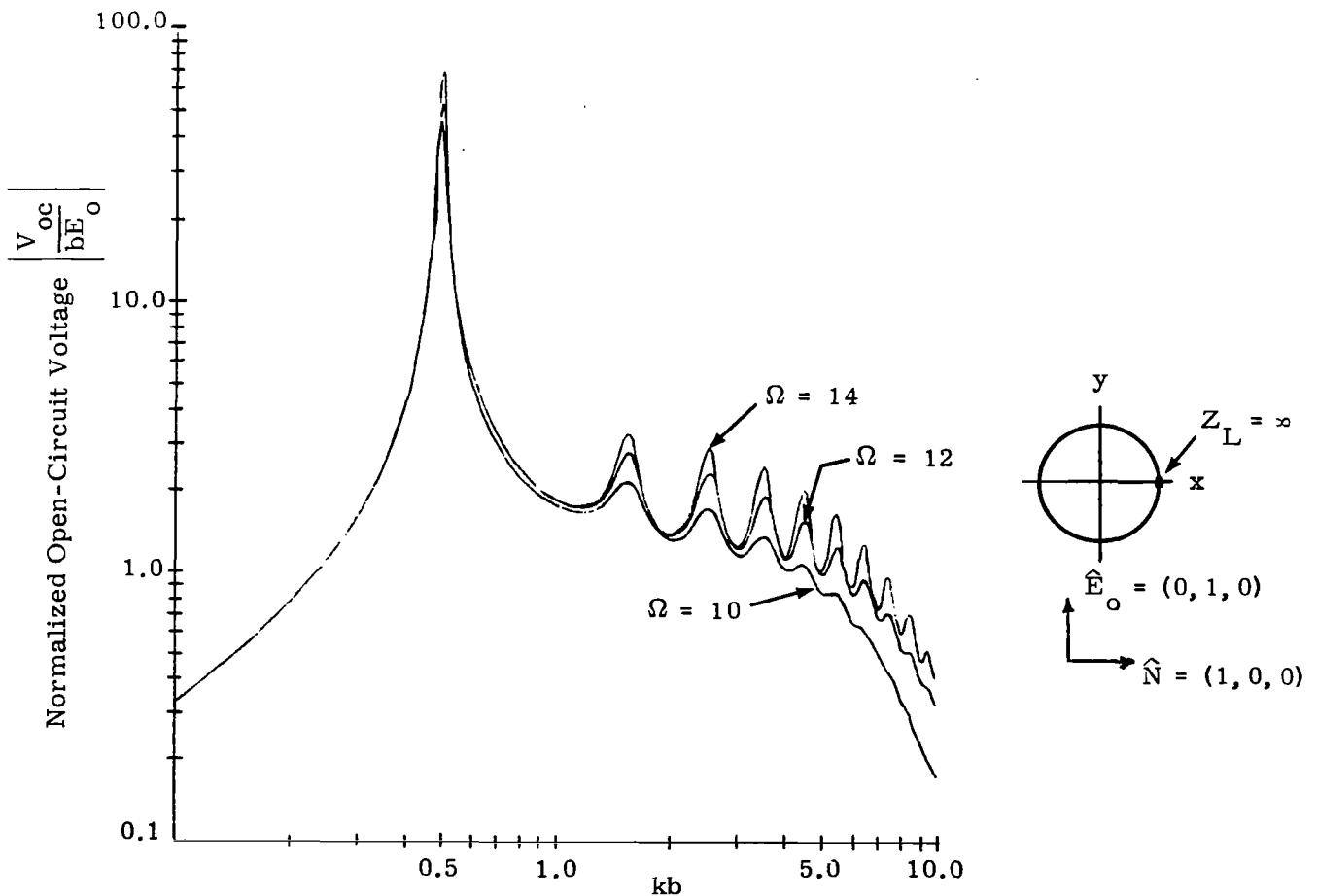


Figure A2. Effect of $\Omega = 2 \ln \frac{2\pi b}{a}$ on the Open-Circuit Voltage Transfer Function

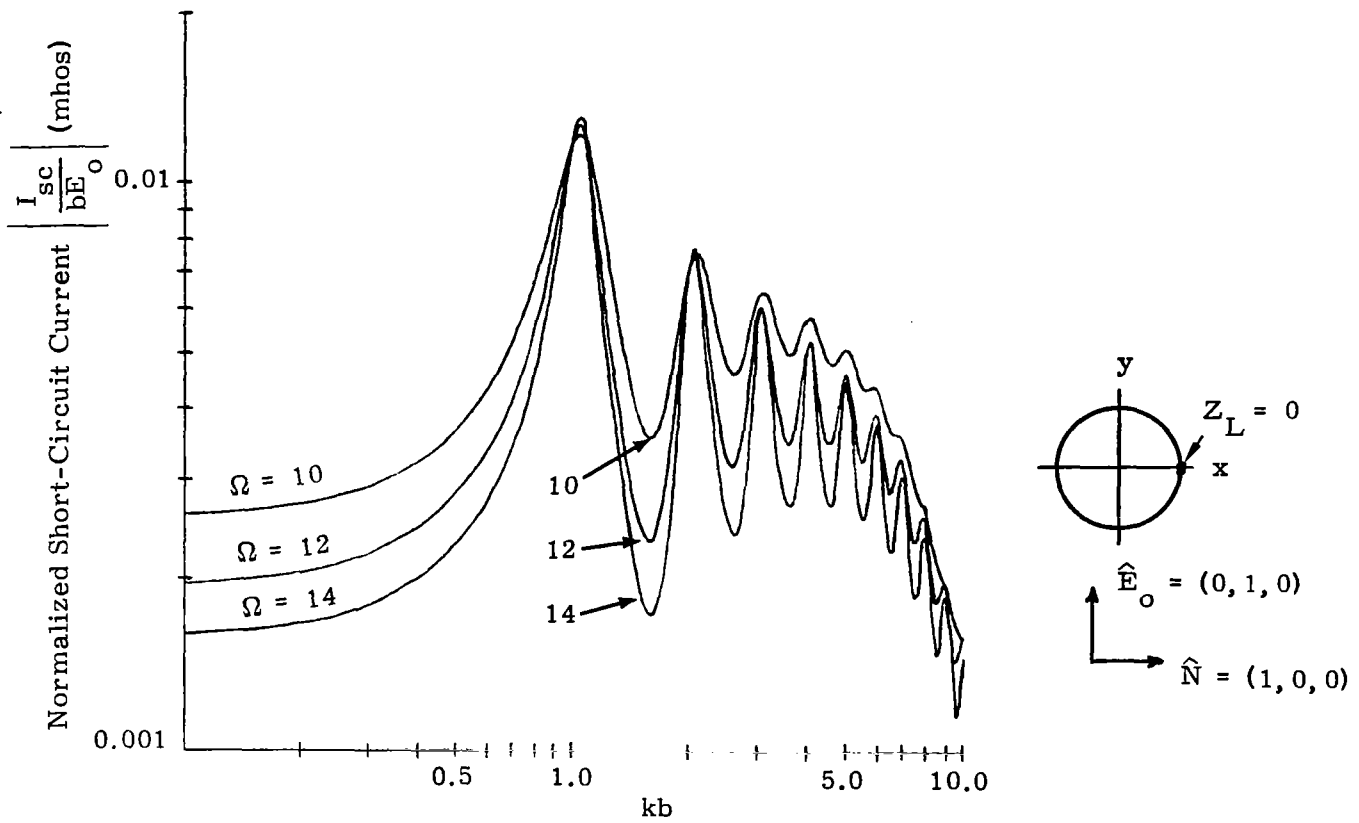


Figure A3. Effect of $\Omega = 2 \ln \frac{2\pi b}{a}$ on the Short-Circuit Current Transfer Function

Effect of Ω on the Transient Response

Figures A4 and A5 are transient responses which correspond (for a unit-step incident plane wave) to the transfer functions of Figures A2 and A3, respectively. These curves are also normalized with respect to b . Using Equations 61 and A1, the load voltage can be written as

$$\begin{aligned} v_L(t) &= \frac{2}{\pi} \int_0^{\infty} \text{Re} \left[bT(kb, \Omega) F(\omega) \right] \cos \omega t d\omega \\ &= \frac{2}{\pi} b \int_0^{\infty} \text{Re} \left[T(kb, \Omega) F\left(kb \frac{c}{b}\right) \right] \cos \left(kb \frac{ct}{b} \right) d(kb) \frac{c}{b}. \end{aligned}$$

If $F(\omega)$, the Fourier transform of the incident electric field, has the form

$$F(\omega) = \frac{1}{j\omega}$$

then

$$v_L(t) = \frac{2}{\pi} b \int_0^\infty \operatorname{Re} \left[T(kb, \Omega) \frac{1}{jkb \left(\frac{c}{b} \right)} \right] \cos \left(kb \frac{ct}{b} \right) d(kb) \frac{c}{b}$$

$$= \frac{2}{\pi} b \int_0^\infty \operatorname{Re} \left[T(kb, \Omega) / jkb \right] \cos \left(kb \frac{ct}{b} \right) d(kb)$$

or

$$v_L(t)/L = g \left(\frac{ct}{b}, \Omega \right)$$

= a function of ct/b and Ω .

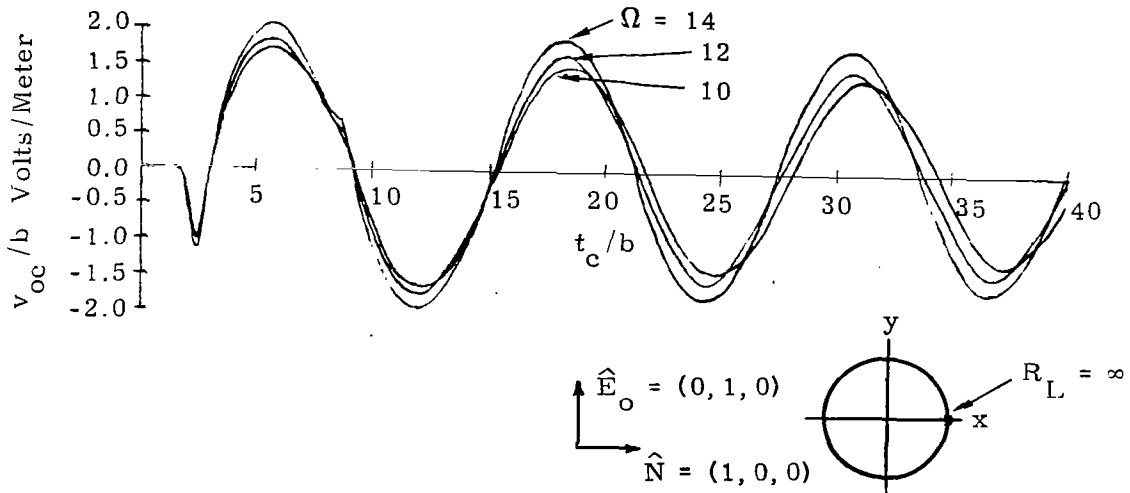


Figure A4. Effect of $\Omega = 2 \ln \frac{2\pi b}{a}$ on the Transient Open-Circuit Voltage

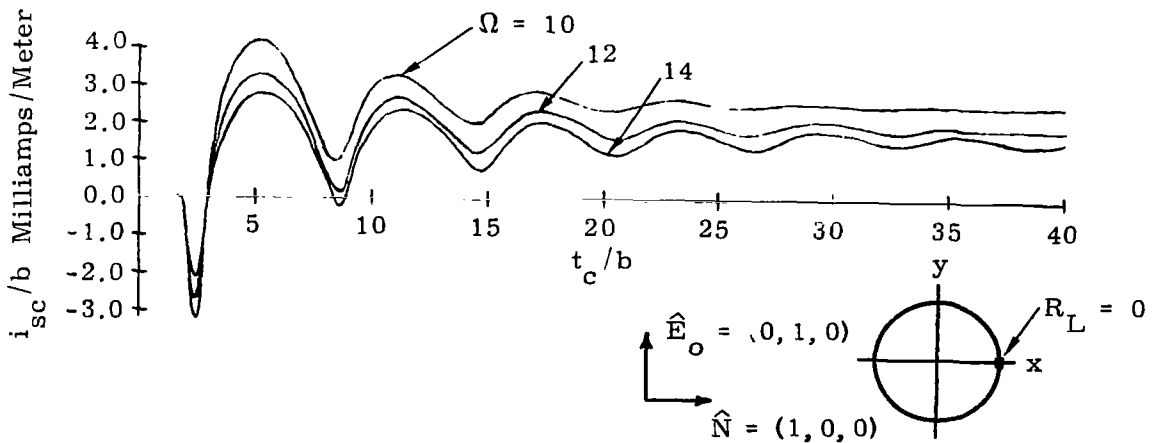


Figure A5. Effect of $\Omega = 2 \ln \frac{2\pi b}{a}$ on the Transient Short-Circuit Current

Effects of Resistive Loading on the Transient Response of a Loop

Figure A6 shows the effects of resistive loading on a loop. It is apparent that, for the loop considered, $R_L \geq 1000$ ohms appears about the same as an open circuit, $500 \text{ ohm} \leq R_L \leq 50 \text{ ohm}$ is a transition region where the loop is nearly critically damped, and $R_L \leq 1 \text{ ohm}$ appears as a short circuit.

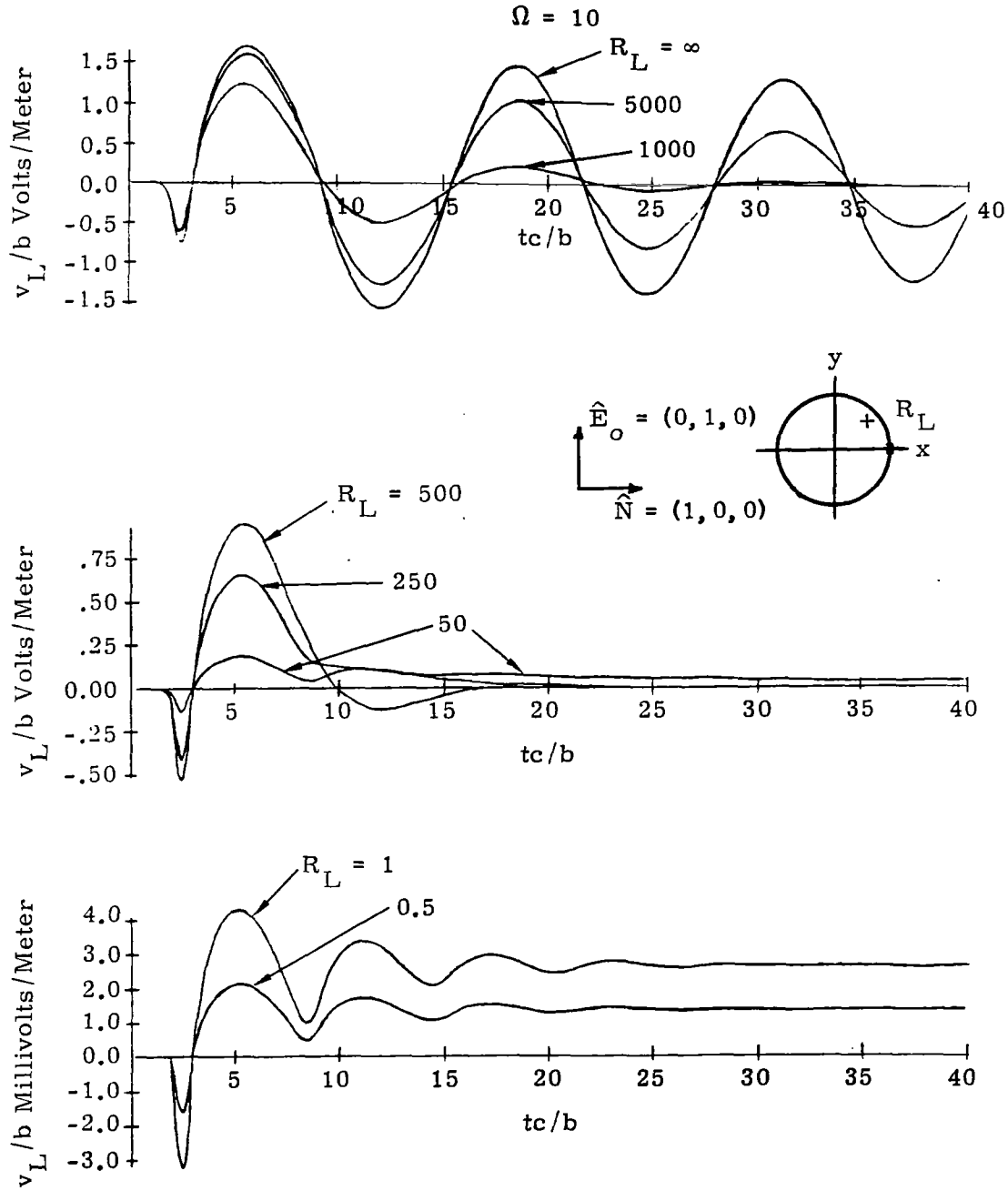


Figure A6. Effects of Resistive Loading on the Transient Response of a Loop

Effects of \hat{E}_o and \hat{N} on the Loop Response

Figures A7 through A10 show the effects of the direction of polarization and the direction of propagation of the electric field on the transient open-circuit voltage and short-circuit current.

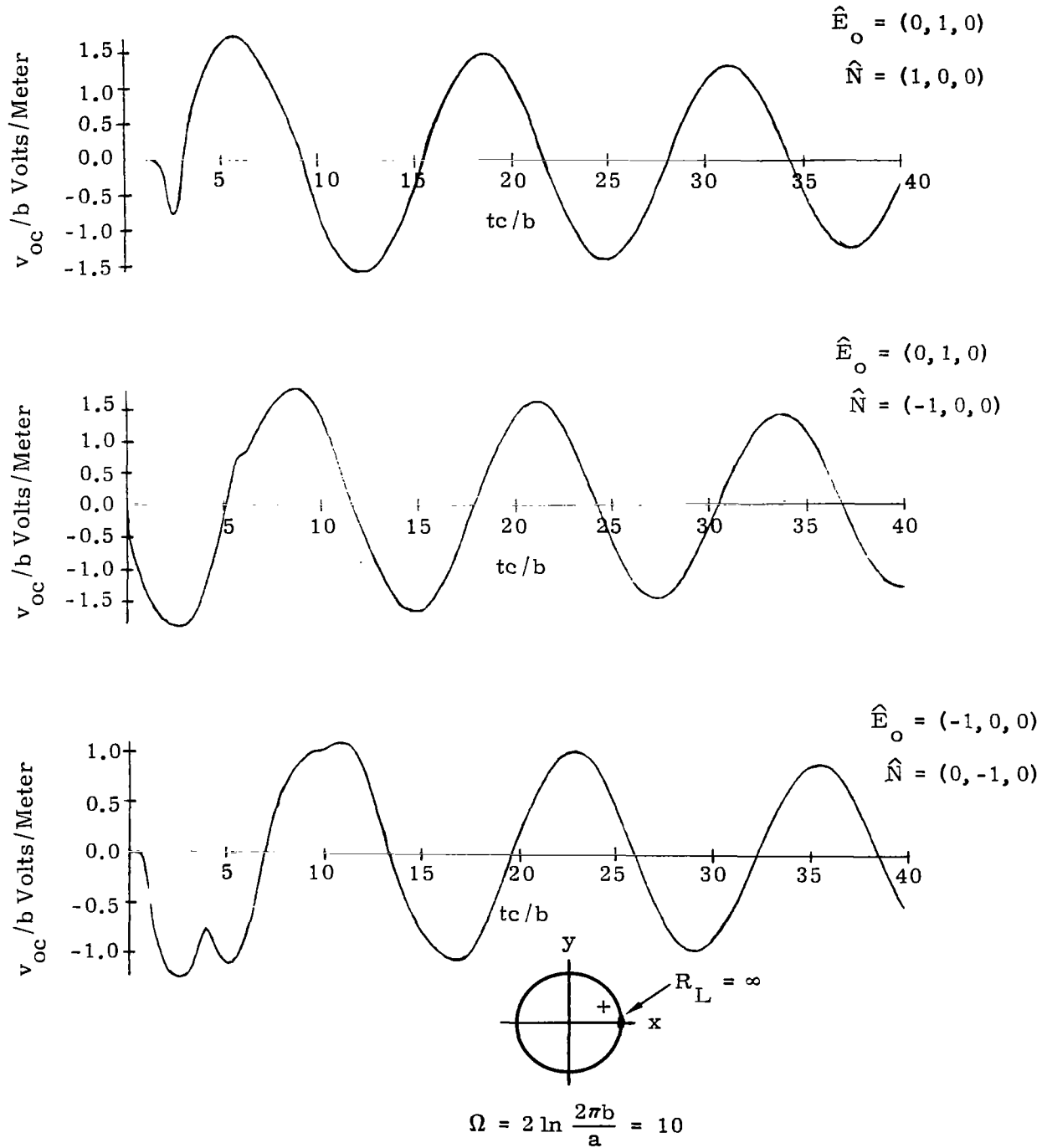
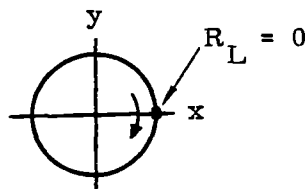
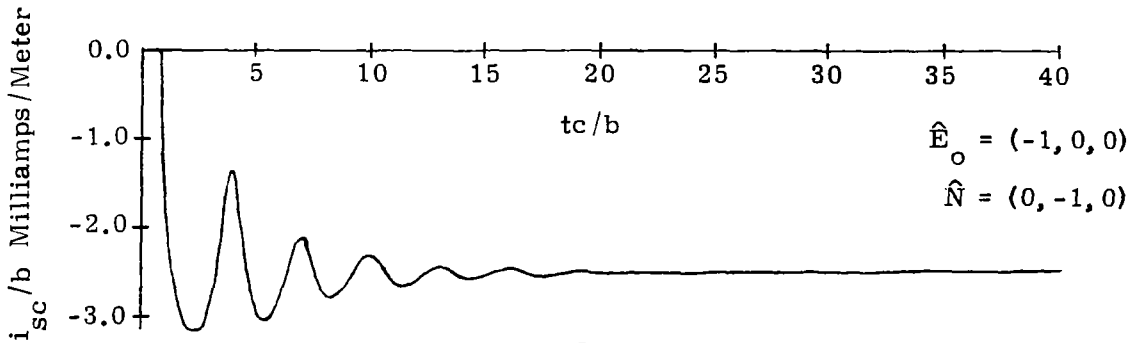
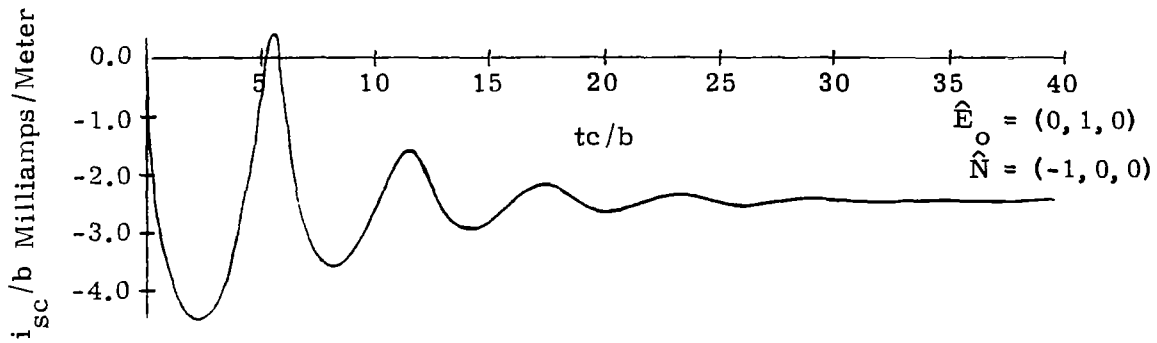
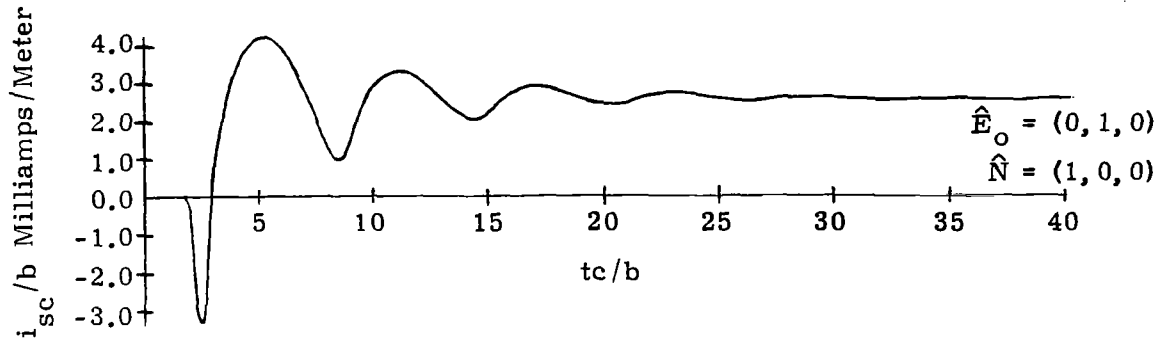


Figure A7. Effects of \hat{E}_o and \hat{N} on the Unit-Step Response of a Loop Antenna (Open-Circuit Voltage)



$$\Omega = 2 \ln \frac{2\pi b}{a} = 10$$

Figure A8. Effects of \hat{E}_o and \hat{N} on the Unit-Step Response of a Loop Antenna (Short-Circuit Current)

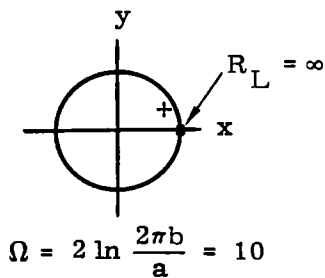
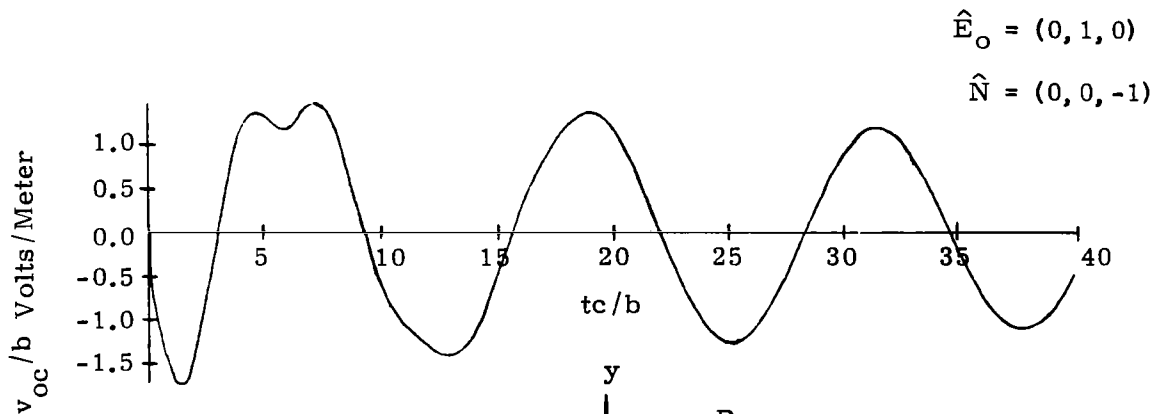
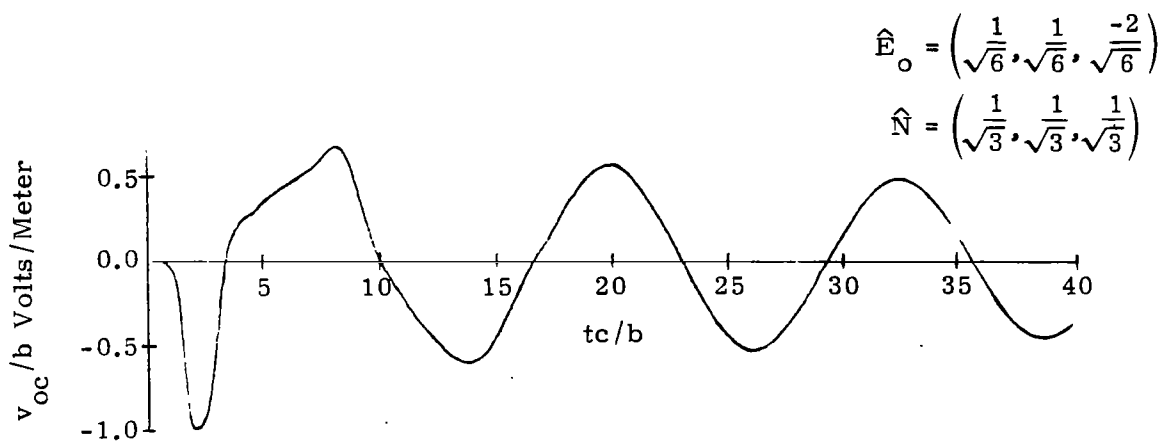
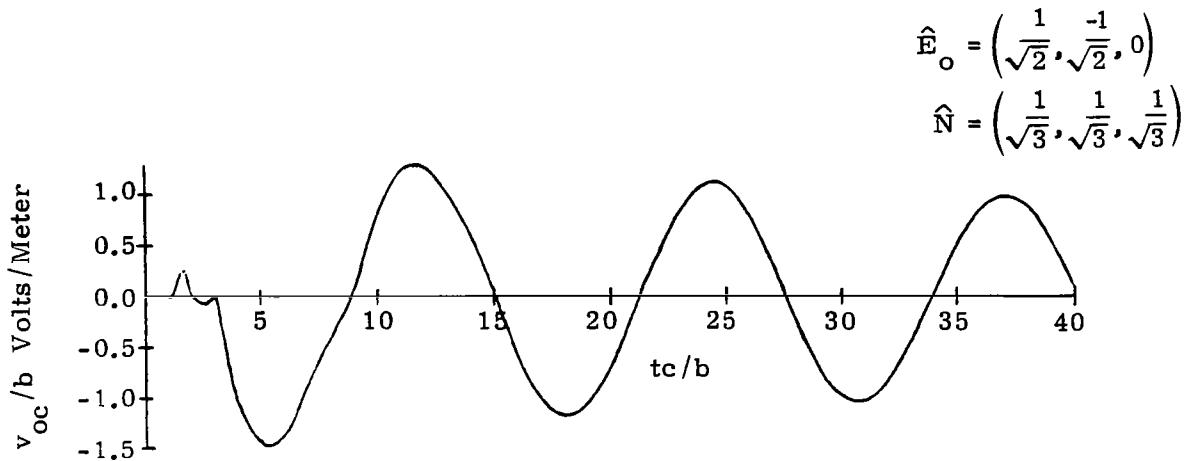


Figure A9. Effects of \hat{E}_o and \hat{N} on the Unit-Step Response of a Loop Antenna (Open-Circuit Voltage)

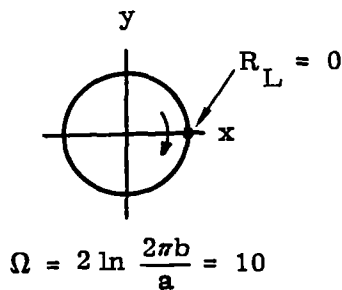
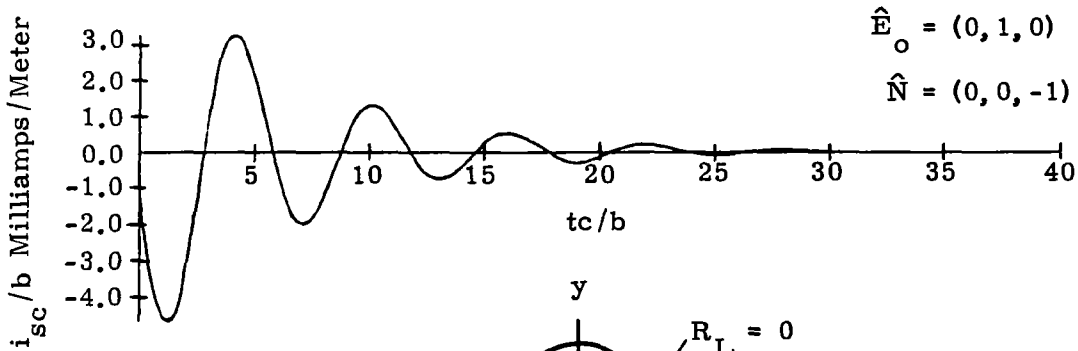
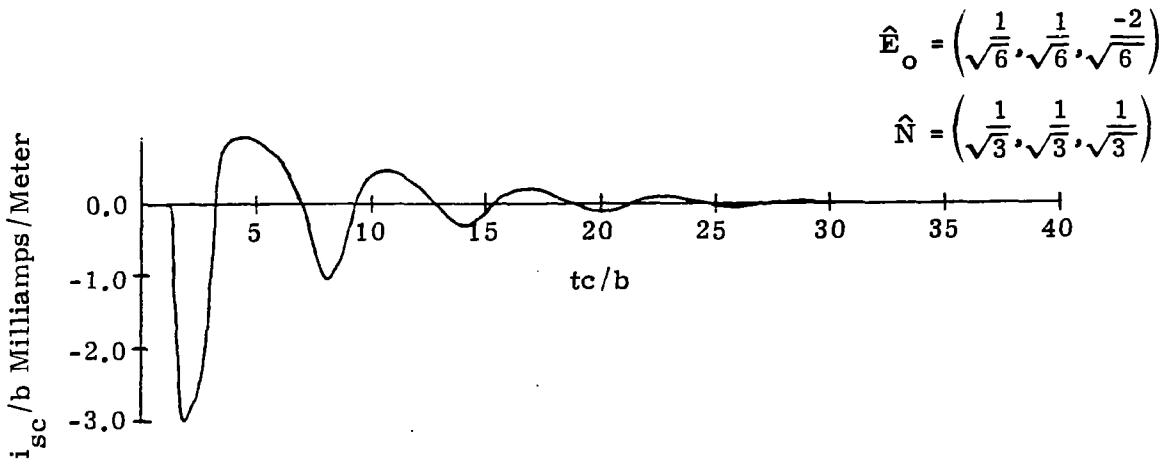
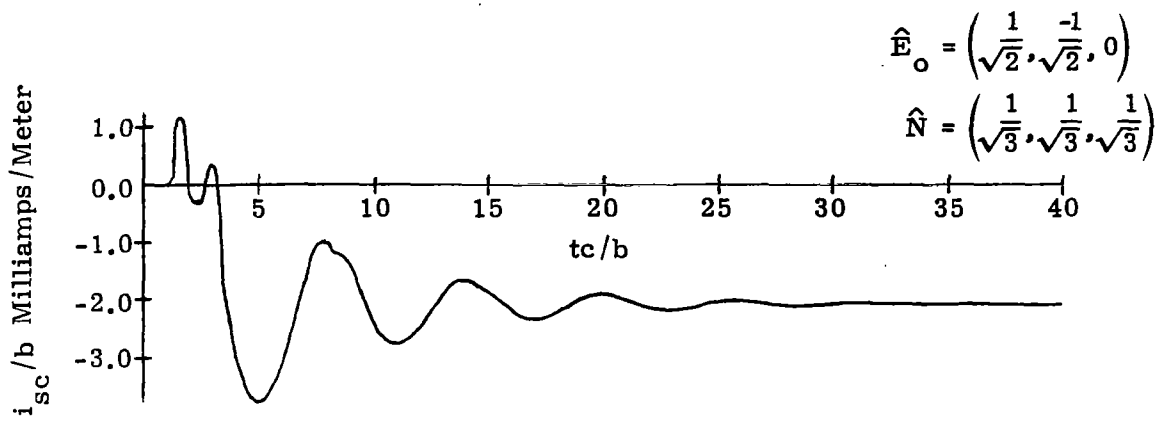


Figure A10. Effects of \hat{E}_0 and \hat{N} on the Unit-Step Response of a Loop Antenna (Short-Circuit Current)

Effect of $\Omega = 2 \ln \frac{2\pi b}{a}$ on the Transient Far Field

The effects of Ω on the radiated far electric field of a loop when driven by a voltage pulse, for an observer at $\theta = \phi = \pi/2$ (see Figure A11), are shown in Figure A12. The drive voltage has the form

$$v(t) = \left\{ 1 - (1 + t/a) e^{-t/a} \right\} e^{-t} u(t) \quad (A3)$$

where

$$a = 1.33 \times 10^{-9} \text{ sec.}$$

The transient radiated electric field cannot be normalized with respect to the radius of the loop b , as was done in the receiving case, because the drive voltage $v(t)$ is not a step function.

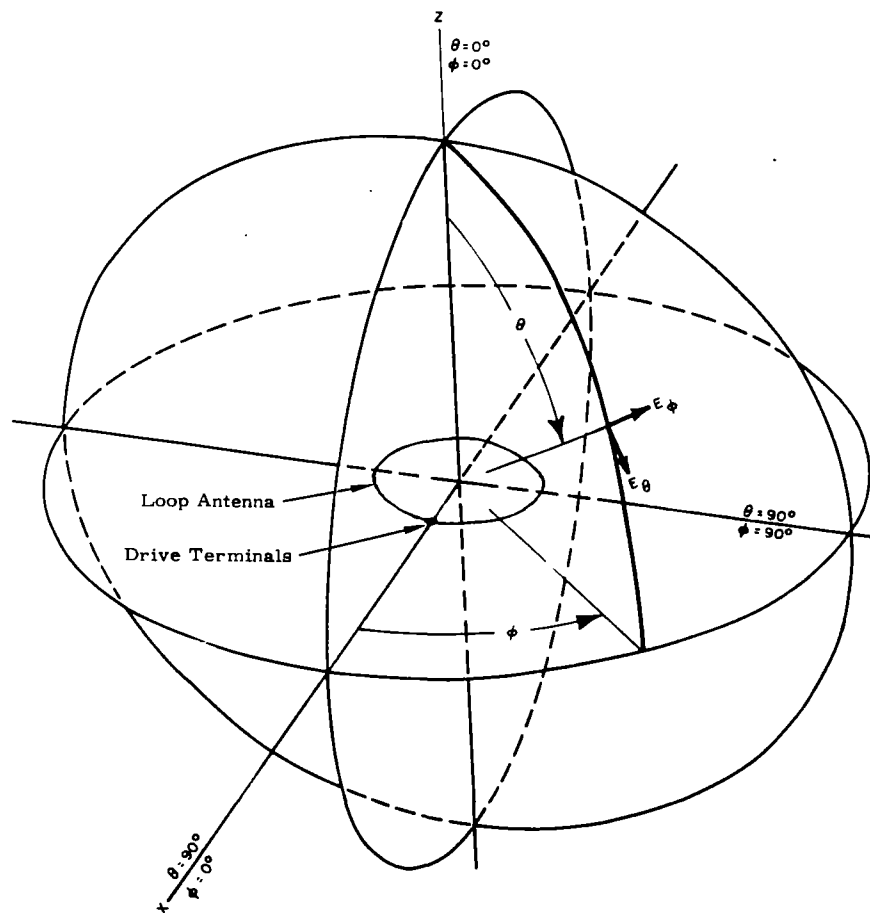


Figure A11. Antenna Coordinate System (the Loop Is in the x-y Plane)

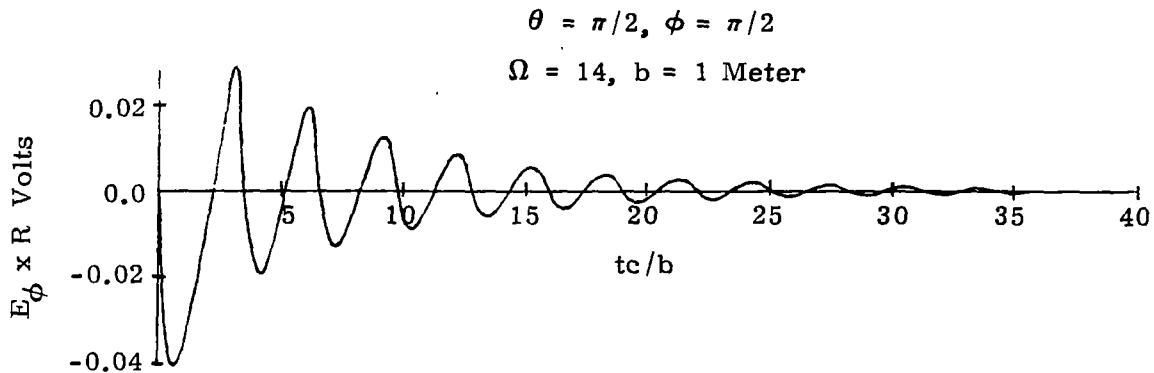
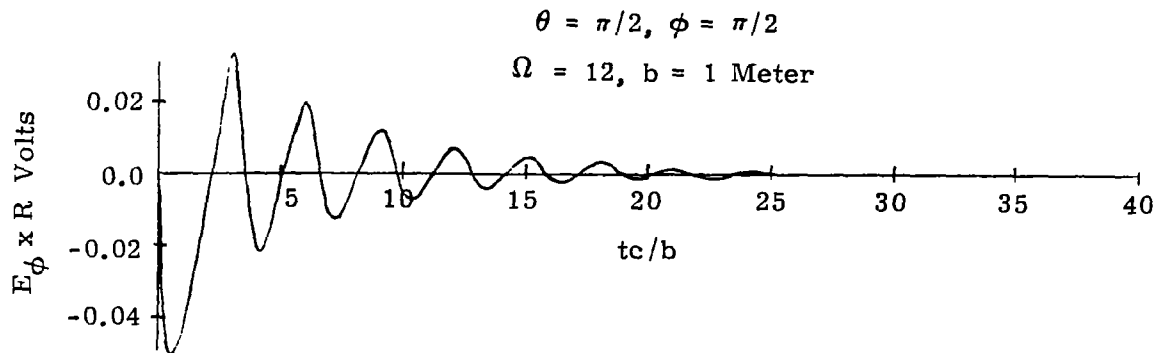
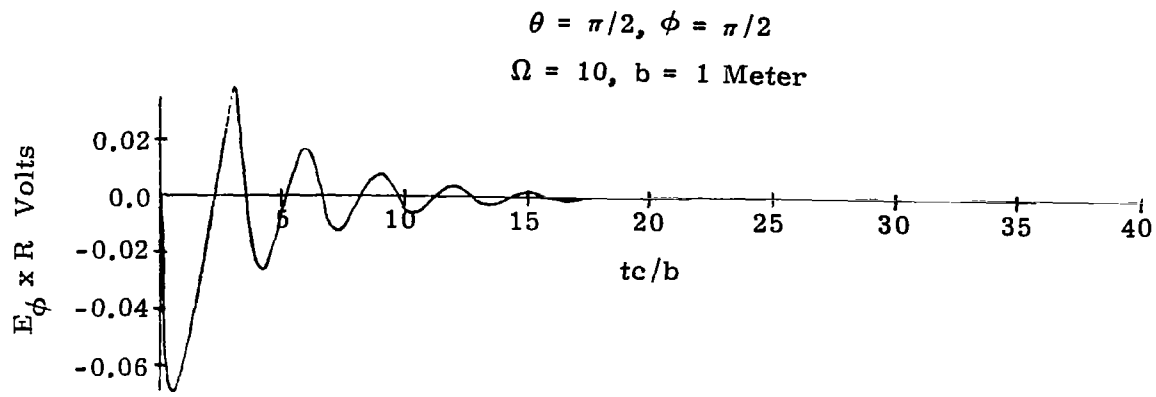
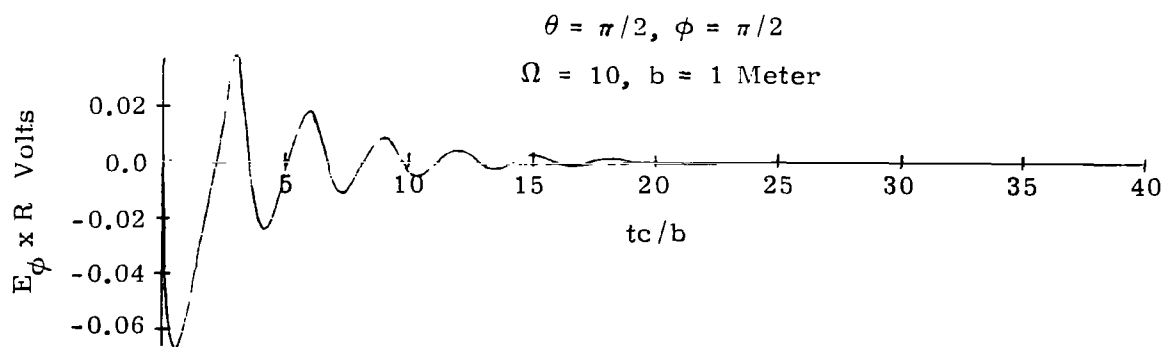
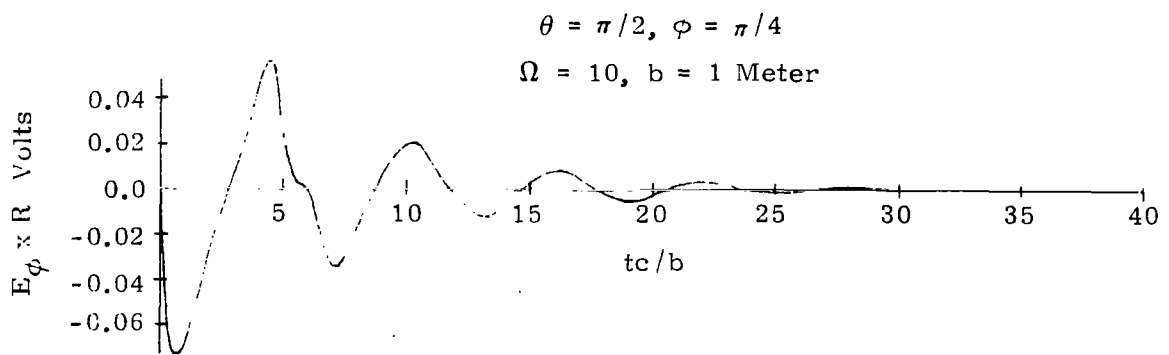
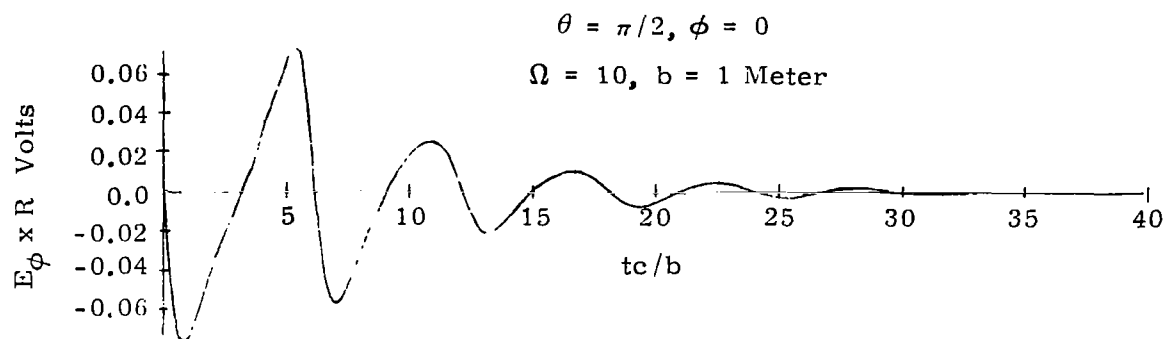


Figure A12. Effect of $\Omega = 2 \ln \frac{2\pi b}{a}$ on the Radiated Electric Field

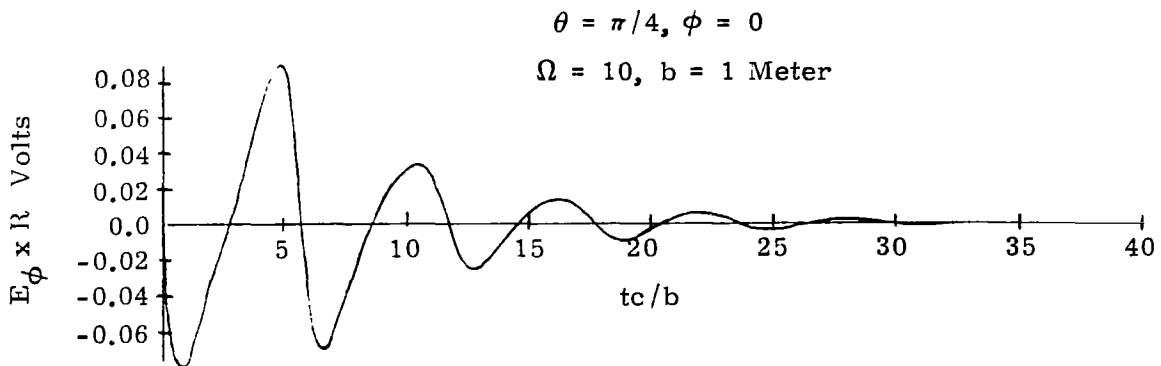
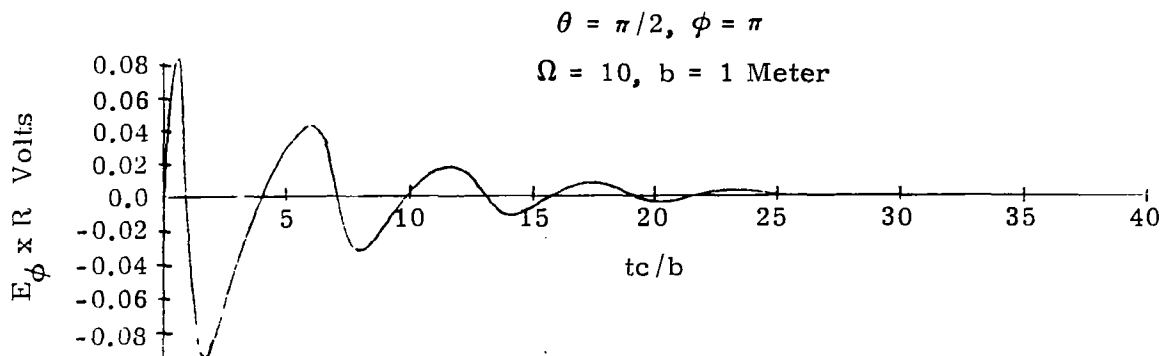
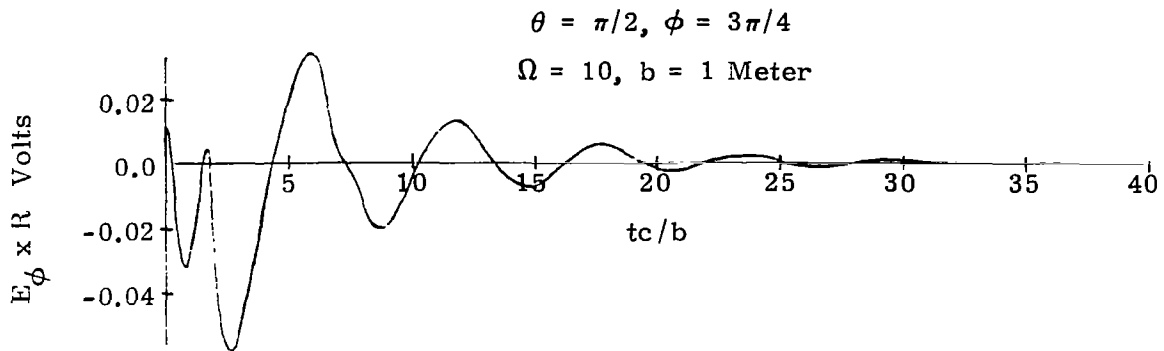
Effects of the Location of the Observer on the Observed Transient Electric Field of a Loop Antenna

Figures A13 through A16 show the observed transient electric field for various observer locations (see Figure A11). For observers in the $\theta = \pi/2$ plane, the θ component of the electric field is zero, and therefore, the total electric field is the ϕ component of the electric field. At $\theta = 0, \phi = \pi/2$, the ϕ component of the electric field is zero.



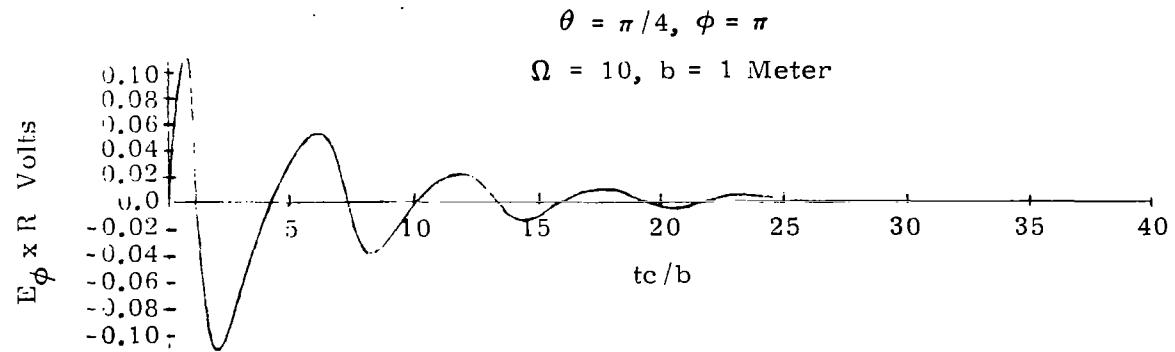
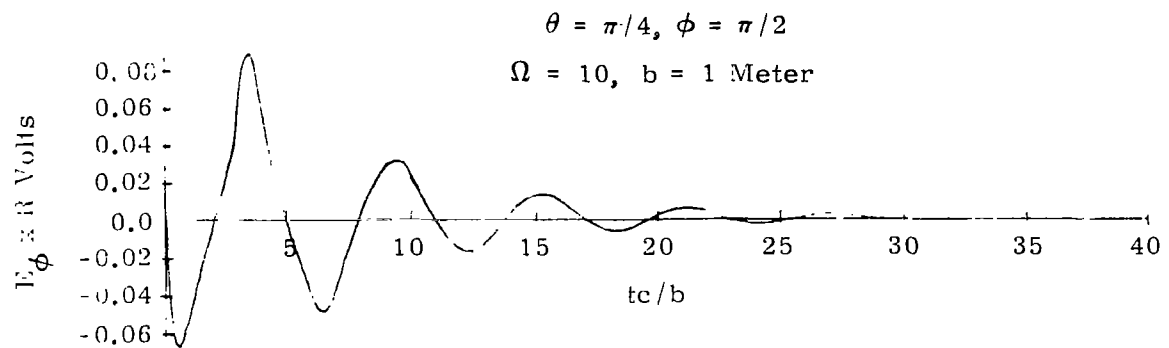
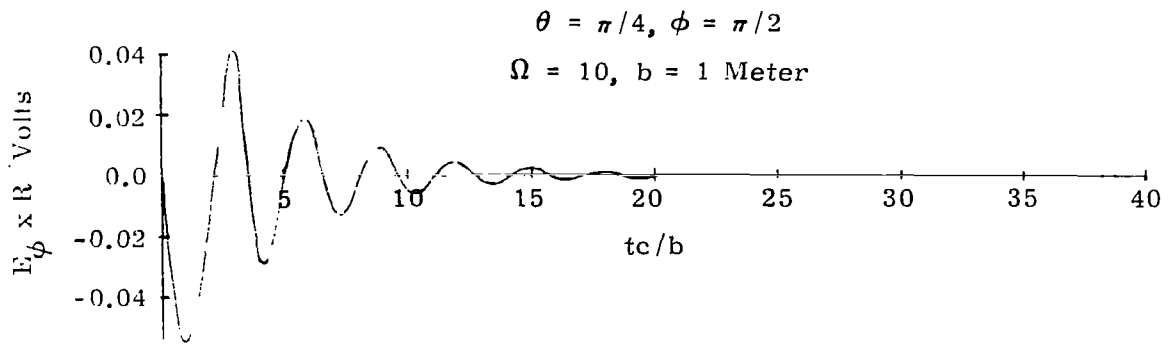
NOTE: The drive voltage waveform is given by Equation A3.
 See Figure A11 for the antenna coordinate system.

Figure A13. Effects of the Location of the Observer on the Observed Transient Electric Field of a Loop Antenna



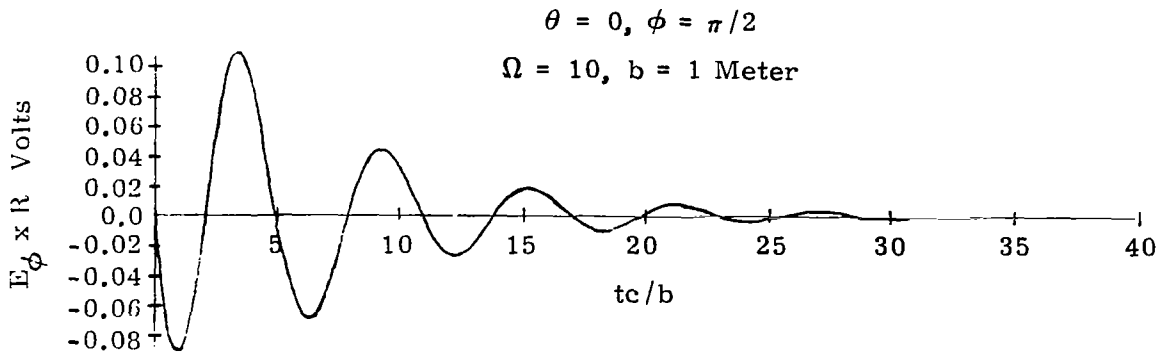
NOTE: The drive voltage waveform is given by Equation A3.
 See Figure A11 for the antenna coordinate system.

Figure A14. Effects of the Location of the Observer on the Observed Transient Electric Field of a Loop Antenna



NOTE: The drive voltage waveform is given by Equation A3.
 See Figure A11 for the antenna coordinate system.

Figure A15. Effects of the Location of the Observer on the Observed Transient Electric Field of a Loop Antenna



NOTE: The drive voltage waveform is given by Equation A3.
 See Figure A11 for the antenna coordinate system.

Figure A16. Effects of the Location of the Observer on the Observed Transient Electric Field of a Loop Antenna

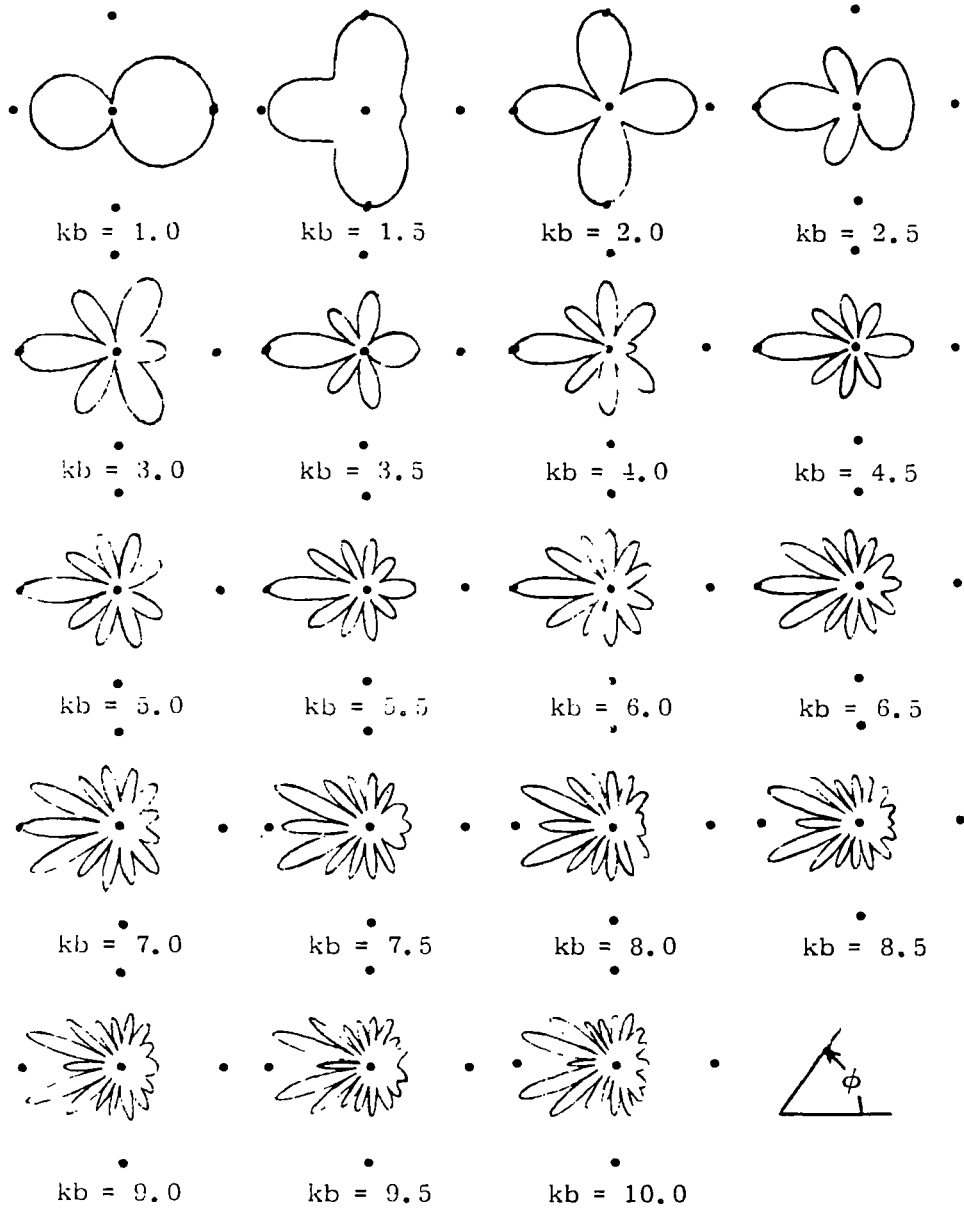
Loop Antenna Patterns

Loop antenna patterns for three different planes are shown as functions of $kb = \frac{\omega b}{c} = \frac{2\pi b}{\lambda}$ in Figures A17 through A21. In the plane $\theta = \pi/2$ and the plane $\phi = 0$, the θ component of the electric field is zero. Therefore, Figures A17 and A18 are also patterns of the total electric field. The electric field in the plane $\phi = \pi/2$ has a ϕ component, Figure A19, and a θ component, Figure A20. Figure A21 shows patterns for the total electric field E_t , where

$$|E_t| = \sqrt{E_\theta E_\theta^* + E_\phi E_\phi^*}$$

and the asterick means the complex conjugate.

The value of the electric field times the distance of the observer from the origin at the angle of greatest electric field intensity is given in Table A1 for each pattern. For example, in Figure A17 for $kb = 4.5$, the value of $|E_\phi|$ at a distance of 10^4 meters from the loop and at $\phi = \pi$ is 6.60×10^{-5} volts/meter if the loop is driven by a 1-volt source.



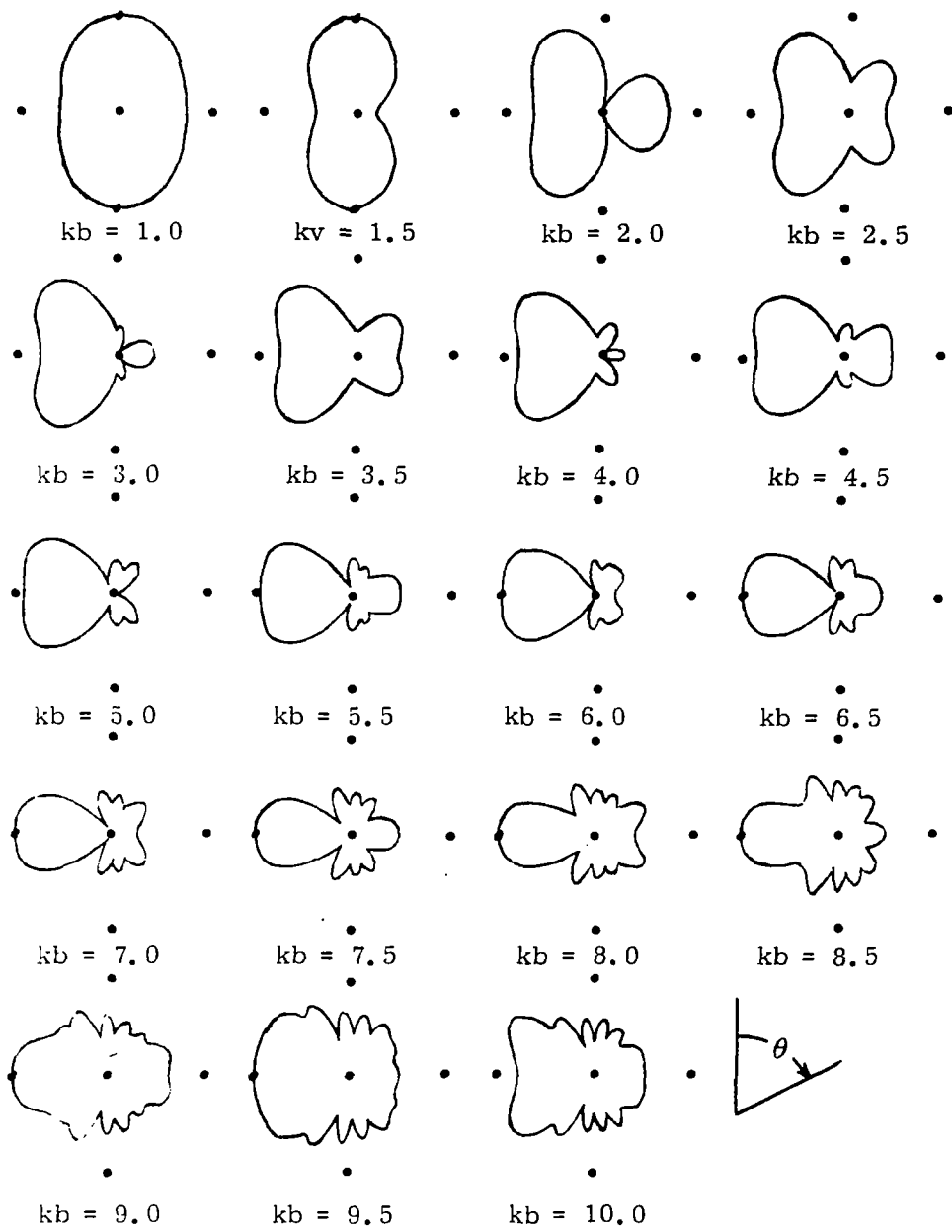
$$\Omega = 10$$

$$\theta = \pi/2 \text{ plane}$$

$$|E_{\phi}|$$

NOTE: See Figure A11 for the antenna coordinate system.

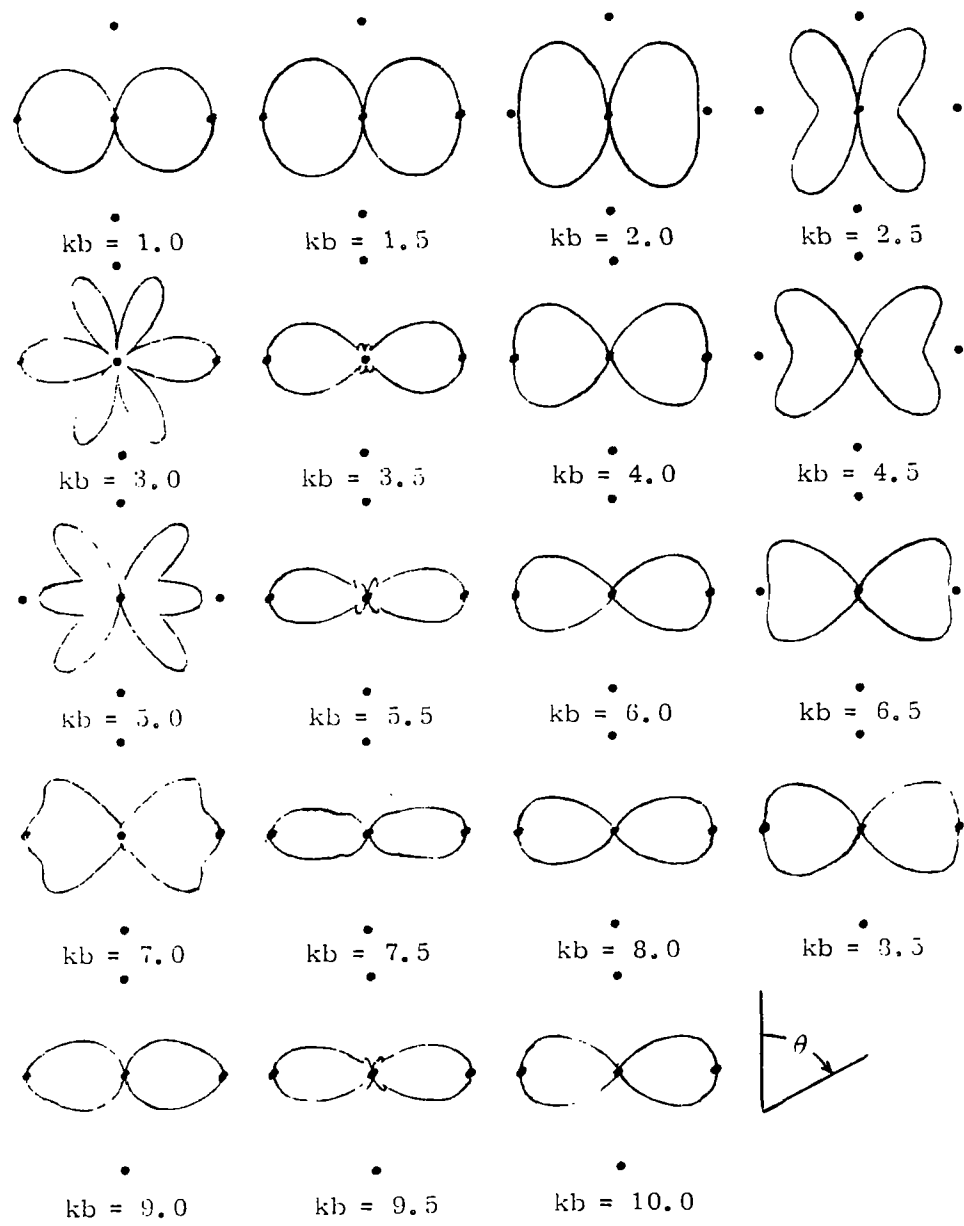
Figure A17. Loop Antenna Patterns



$\Omega = 10$
 $\phi = 0$ plane
 $|E_{\phi}|$

NOTE: See Figure A11 for the antenna coordinate system.

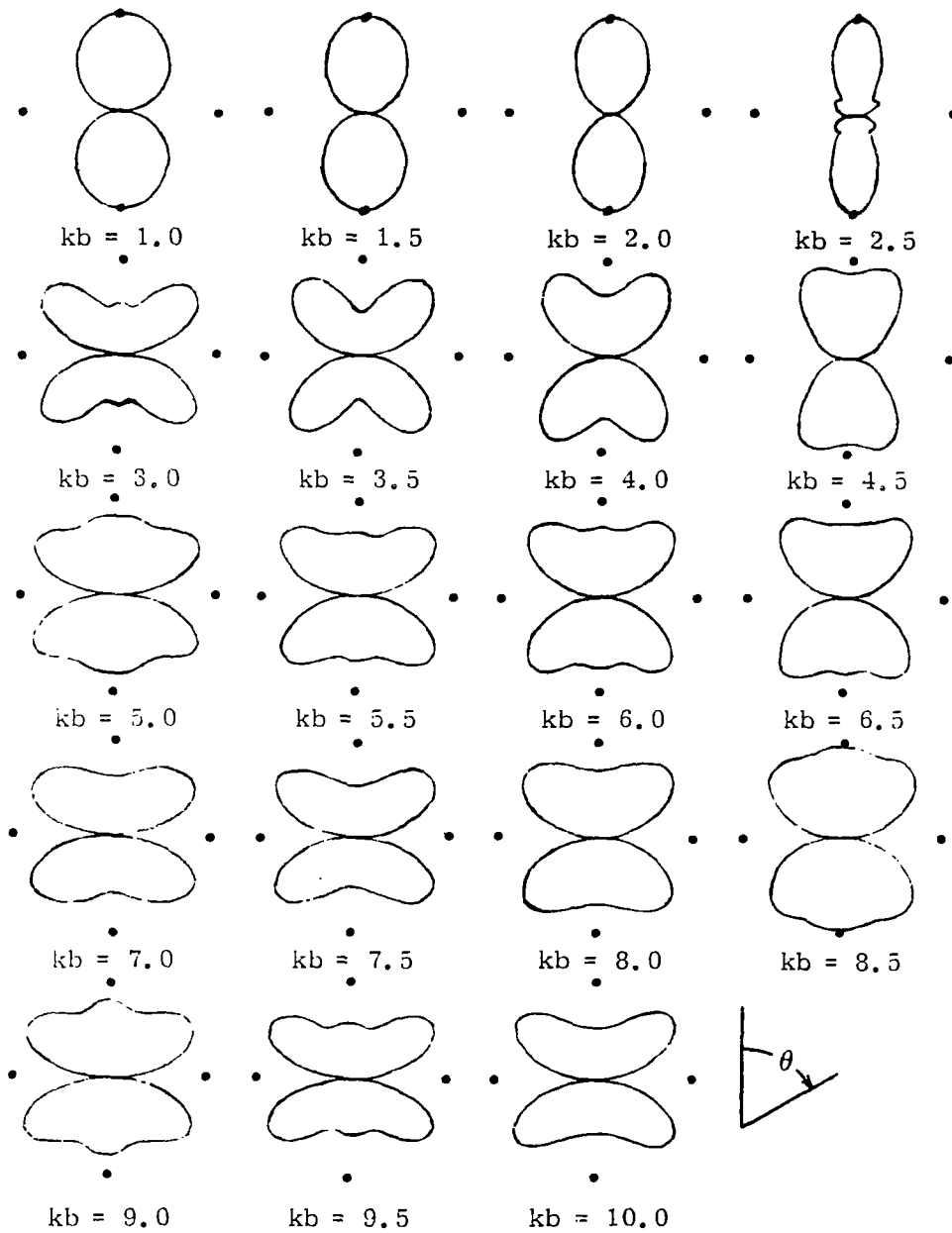
Figure A18. Loop Antenna Patterns



$\Omega = 10$
 $\phi = \pi/2$ plane
 $|E_{\phi}|$

NOTE: See Figure A11 for the antenna coordinate system.

Figure A19. Loop Antenna Patterns



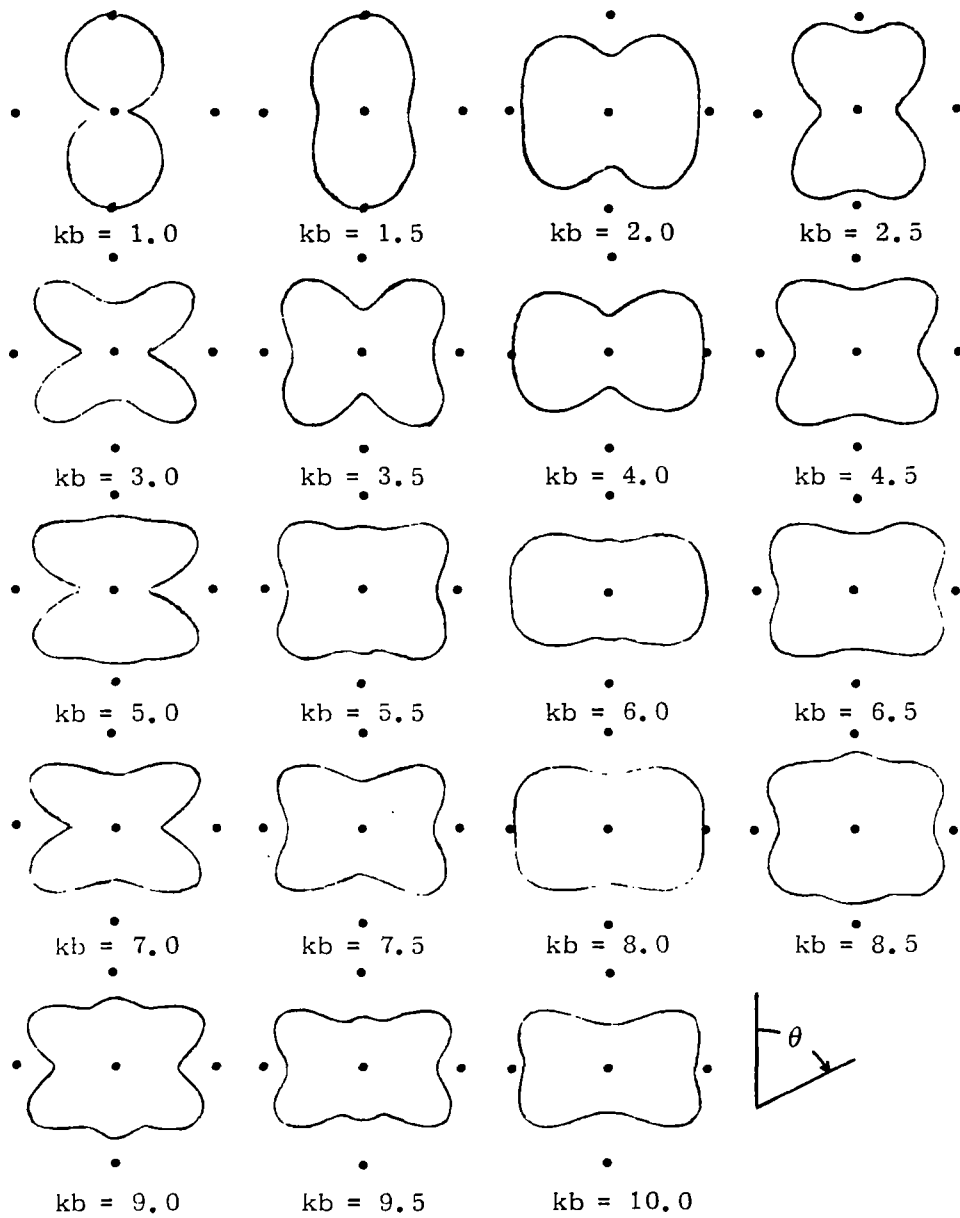
$$\Omega = 10$$

$$\phi = \pi/2 \text{ plane}$$

$$|E_{\theta}|$$

NOTE: See Figure A11 for the antenna coordinate system.

Figure A20. Loop Antenna Patterns



$$\Omega = 10$$

$$\phi = \pi/2 \text{ plane}$$

$$|E_t| = \sqrt{E_\theta E_\theta^* + E_\phi E_\phi^*}$$

NOTE: See Figure A11 for the antenna coordinate system.

Figure A21. Loop Antenna Patterns

TABLE A1

Values of the Electric Field in Volts/Meter, at the Angle of Greatest Electric Field Intensity Times the Distance of the Observer from the Origin

| kb | Figure | | | | |
|------|--------|-------|--------|-------|-------|
| | A17 | A18 | A19 | A20 | A21 |
| 1.0 | 0.411 | 0.587 | 0.0859 | 0.586 | 0.586 |
| 1.5 | 0.184 | 0.398 | 0.180 | 0.393 | 0.393 |
| 2.0 | 0.426 | 0.576 | 0.460 | 0.271 | 0.472 |
| 2.5 | 0.363 | 0.536 | 0.246 | 0.211 | 0.259 |
| 3.0 | 0.543 | 0.698 | 0.118 | 0.346 | 0.348 |
| 3.5 | 0.537 | 0.666 | 0.292 | 0.389 | 0.404 |
| 4.0 | 0.670 | 0.782 | 0.472 | 0.292 | 0.488 |
| 4.5 | 0.660 | 0.733 | 0.298 | 0.245 | 0.329 |
| 5.0 | 0.751 | 0.801 | 0.145 | 0.326 | 0.343 |
| 5.5 | 0.732 | 0.755 | 0.324 | 0.421 | 0.429 |
| 6.0 | 0.773 | 0.783 | 0.476 | 0.345 | 0.483 |
| 6.5 | 0.726 | 0.727 | 0.313 | 0.283 | 0.363 |
| 7.0 | 0.733 | 0.733 | 0.179 | 0.352 | 0.391 |
| 7.5 | 0.771 | 0.668 | 0.346 | 0.455 | 0.475 |
| 8.0 | 0.829 | 0.637 | 0.471 | 0.406 | 0.490 |
| 8.5 | 0.874 | 0.564 | 0.329 | 0.341 | 0.414 |
| 9.0 | 0.898 | 0.528 | 0.266 | 0.393 | 0.429 |
| 9.5 | 0.904 | 0.486 | 0.399 | 0.483 | 0.524 |
| 10.0 | 0.930 | 0.596 | 0.477 | 0.460 | 0.551 |

APPENDIX B
Computer Programs

APPENDIX B

Computer Programs

Listed in this appendix are the computer programs which were used to calculate the curves of Appendix A. Each program contains comment cards which explain the program's use and the input and output variables. Also listed are the subprograms which are called from the four main programs. The subprograms used in each main program are listed in the main programs.


```

PROGRAM LOOP RE(INPUT,OUTPUT,TAPE10)
C THIS PROGRAM COMPUTES THE VOLTAGE ACROSS THE LOAD IMPEDENCE OF A LOOP ANTENNA
C WHEN ILLUMINATED BY A TRANSIENT ELECTROMAGNETIC PLANE WAVE. LOAD CURRENTS CAN
C BE CALCULATED BY A SMALL CHANGE AS INDICATED IN A LATER COMMENT CARD.
C THE LOOP IS IN THE X-Y PLANE AT Z=0 AND IS DRIVEN AT PHI=0. A=THE WIRE RADIUS
C AND B=THE LOOP RADIUS, BOTH IN METERS.
C
C SUBROUTINES OR SUBFUNCTIONS TO BE USED WITH THIS PROGRAM ARE
C     SUBROUTINE VOCZA
C     SUBROUTINE BETAN
C     SUBROUTINE RR
C     SUBROUTINE SICOINT
C     SUBFUNCTION E
C     SUBFUNCTION ZL
C ALL DIMENSIONED VARIABLES MUST BE LEFT AT THEIR PRESENT SIZE.
COMMON/A/ VO(301),IS(301),VE(301),VT(214,8),VSPACE(283)
COMMON/B/ AOB,BK,GAMMA1,JBK,AOROL,FRRB
COMMON/C/ EX,EY,EZ,L,M,N,B,ERR,ER,NCALL
COMPLEX JBK,ZA,VOC,VE,ZLW,ZL,E
REAL L,M,N,IS
DIMENSION BKM(301),ZA(301),VOC(301),TA(6)
DATA PI,C/3.1415927,3.F8/
NCALL=0
AOBOL=-1.
READ 14,NIMP,NFUNCT
C NIMP IS THE NUMBER OF LOAD IMPEDENCES TO BE USED FOR EACH DRIVE FUNCTION.
C NFUNCT IS THE NUMBER OF DIFFERENT DRIVE FUNCTIONS TO BE USED .
  14 FORMAT(2I5)
  READ 1,EX,EY,EZ,L,M,N,A,B
C EX,EY,AND EZ ARE THE COMPONENTS OF THE INCIDENT ELECTRIC FIELD. MUST HAVE
C EX**2+EY**2+EZ**2=1----L,M,AND N ARE COMPONENTS OF THE UNIT VECTOR POINTING
C IN TNE DIRECTION OF PROPAGATION OF THE PLANE WAVE. MUST HAVE L**2+M**2+N**2=1
C AND EX*L+EY*M+EZ*N=0. A=THE WIRE RADIUS AND B=THE LOOP RADIUS,BOTH IN METERS.
  1 FORMAT(8E10.0)
  PRINT 9,EX,EY,EZ,L,M,N,A,B
  PRINT 10
  ERFB=0.
  AOB=(A/B)**2
  ERR=1.E-3
  EXA=EXP(1.)
  COB=C/B
  BOC=B/C
  BKM(1)=BOC*1.E-3
  BK=BOC*3.140327711/EXA
  DO 2 I=1,19
  DBK=BK/6.
  JA=6*(I-1)
  DO 3 IA=2,7
  JB=JA+IA
  3 BKM(JB)=BKM(JB-1)+DBK
  2 BK=BK*EXA
  DO 25 I=116,135
  25 BKM(I)=BKM(I-1)+0.01
  DBK=(10.-BKM(135))/166.
  DO 4 I=136,301

```

```

4 BKM(I)=BKM(I-1)+DBK
DO 5 I=1,301
RK=BKM(I)
CALL VOCZA(VOC(I),ZA(I))
5 CONTINUE
PRINT 9,VOC
C VOC(I)=THE VALUE OF THE OPEN CIRCUIT VOLTAGE TRANSFER FUNCTION AT BKM(I).
PRINT 10
PRINT 9,ZA
C ZA(I)=THE VALUE OF THE ANTENNA IMPEDENCE AT BKM(I).
PRINT 10
PRINT 9,BKM
C BKM(I) IS A MATRIX OF THE VALUE OF  $BK=2*PI*FREQUENCY*B/(THE\ VELOCITY\ OF\ LIGHT)$ 
PRINT 10
9 FORMAT(10E13.4)
10 FORMAT(////////)
CBPI=-2.*COB/PI
R=1.00475
DT=0.15
VO(1)=0.
DO 11 I=2,201
VO(I)=VO(I-1)+DT
11 DT=DT*R
DO 12 ID=1,NFUNCT
DO 18 IB=1,8
DO 18 IA=1,214
18 VT(IA,IB)=0.
DO 13 IA=1,301
13 VE(IA)=VOC(IA)*E(BKM(IA)*COB,IB)
DO 24 IA=1,NIMP
DO 16 IB=1,301
ZLW=ZL(W,IA)
C LOAD CURRENT CAN BE CALCULATED BY REPLACING THE NEXT FORTRAN STATEMENT BY
C 16 IS(IB)=REAL(VE(IB)/(ZA(IB)+ZLW))
16 IS(IB)=REAL(VE(IB)*ZLW/(ZA(IB)+ZLW))
DO 15 IB=1,201
DO 17 IC=1,109,6
CALL SICOINT(BKM(IC),BKM(IC+6),6,VO(IB),IS(IC),VSPACE,V1,V2,V3,V4)
17 VT(IB,IA)=VT(IB,IA)+V1
CALL SICOINT(BKM(115),BKM(135),20,VO(IB),IS(115),VSPACE,V1,V2,V3,V
14)
VT(IB,IA)=VT(IB,IA)+V1
CALL SICOINT(BKM(135),BKM(301),166,VO(IB),IS(135),VSPACE ,V1,V2,V3
1,V4)
15 VT(IB,IA)=(VT(IB,IA)+V1)*CBPI
24 CONTINUE
PRINT 9,VT
C VT(I)=THE VALUE OF THE TRANSIENT LOAD VOLTAGE AT THE TIME SUCH THAT
C  $TIME*(THE\ VELOCITY\ OF\ LIGHT)/B=VO(I)$ .
PRINT 10
PRINT 9,VO
PRINT 10
12 CONTINUE
END

```

```

PROGRAM LOOP TR(INPUT,OUTPUT,TAPFIC)
C THIS PROGRAM COMPUTES THE TRANSIENT FAR FIELD THETA AND PHI COMPONENTS OF THE
C RADIATED ELECTRIC FIELD DUE TO A LOOP DRIVEN BY A TRANSIENT VOLTAGE. THE LOOP
C IS IN THE X-Y PLANE AT Z=0 AND IS DRIVEN AT PHI=0. A=THE WIRE RADIUS AND
C R=THE LOOP RADIUS, BOTH IN METERS.
C
C SUBROUTINES OR SUBFUNCTIONS TO BE USED WITH THIS PROGRAM ARE
C     SUBROUTINE FAR E
C     SUBROUTINE RETAN
C     SUBROUTINE RR
C     SUBROUTINE SICOINT
C     SUBFUNCTION E
C
C THE DIMENSIONS ARE---EP(N1),EPT(NTP),ETT(NTP),T(NTP+1). HERE N1=N+1 AND
C NTP=NT+13, N AND NT ARE READ INTO THE PROGRAM.
  DIMENSION EP(301),ET(301)
  DIMENSION EPT(301),ETT(301),T(302)
  COMMON/A/EPG(3199)
  COMMON/B/AOB,BK,GAMMA1,JKB,AOBOL,ERRB
  COMMON/C/THETA,PHI,CON,M,ERR,ETHETA,EPHI,AORO,BKO,ERROR
  TYPE COMPLEX JKB, ETHETA,EPHI,E,CONST,J,EW
  DATA PI,C,J/3.1415927,3.E8,(0.,1.)/
  AORO=-1.
  BKO=-1.
  AOBOL=-1.
  READ 13,NRUN
C NRUN IS THE NUMBER OF TRANSIENT WAVEFORMS TO BE CALCULATED.
  13 FORMAT(I3)
  DO 5 L=1,NRUN
  READ 1,R,THETA,PHI,A,B,DT,NT,N
C (R,THETA,PHI) ARE THE COORDINATES OF THE OBSERVER.
C A AND B ,IN METERS, ARE THE RADII OF THE WIRE AND THE LOOP, RESPECTIVELY.
C NT IS THE NUMBER OF TIME POINTS AT WHICH THE TRANSIENT RADIATED FIELD IS TO BE
C EVALUATED. DT IS THE INTERVAL BETWEEN TIME POINTS.
C N+1 IS THE NUMBER OF POINTS AT WHICH THE TRANSFER FUNCTION IS EVALUATED ON THE
C INTERVAL 0.1 .LE. BK .LE. 10.
  PRINT 9,R,THETA,PHI,A,B,DT,NT,N
  PRINT 8
  1 FORMAT(6E10.0,2I5)
  7 FORMAT(10E13.4)
  8 FORMAT(////////)
  9 FORMAT(6E17.6,2I10)
  ERROR=0.
  ERRB=0.
  BK=0.1
  DBK=9.9/N
  AOB=(A/B)**2
  CON=-0.25/(PI*PI*R)
  ERR=1.E-3
  N1=N+1
  COB=C/B
  CONS=2.*COB/PI
  SICO=SIN(THETA)*COS(PHI)
  DO 2 I=1,N1
  JKB=J*BK

```

```

M=3.*BK
IF(M.LT.5) M=5
CALL FAR E
W=COR*BK
FW=F(W,2)*CEXP(-JKB*SICO)
ET(I)=REAL(ETHETA*EW)
EP(I)=REAL(EPhi*FW)
2 BK=BK+DBK
T(1)=0.
DT=DT*COR
DO 3 I=1,NT
CALL SICOINT(0.1,10.,N,T(I),ET,EP,ETT(I),UN,EPT(I),UM)
T(I+1)=T(I)+DT
ETT(I)=ETT(I)*CONS
3 EPT(I)=EPT(I)*CONS
AA=(-B*GAMMA1*SIN(THETA)/(2.*PI*R*C))*COB
EPT(1)=EPT(1)+0.1*AA
DO 4 I=2,NT
4 EPT(I)=EPT(I)+AA*SIN(0.1*T(I))/T(I)
PRINT 7,ERROR,ERRB
C ERROR IS RETURNED FROM SUBROUTINE FAR E. IF ERROR=0 THE NUMERICAL INTEGRATION
C IN SUBROUTINE FAR E IS ACCURATE TO ATLEAST 3 SIGNIFICANT FIGURES. IF ERROR=
C X*10**(-N) .LT. X .LT. 10. THE INTEGRATION IS ACCURATE TO ATLEAST N-1
C SIGNIFICANT FIGURES.
C ERRB IS SIMILAR TO ERROR EXCEPT THAT IT IS RETURNED FROM SUBROUTINE BETAN.
PRINT 8
PRINT 7,ETT
C ETT(I)=THE VALUE OF THE THETA COMPONENT OF THE TRANSIENT ELECTRIC FIELD AT
C T(I). EPT(I)=THE PHI COMPONENT.
PRINT 8
PRINT 7,EPT
5 CONTINUE
END

```

```

PROGRAM CURR(INPUT,OUTPUT,TAPE10)
C THIS PROGRAM COMPUTES THE TRANSIENT TRANSMITTING CURRENT DISTRIBUTION ON A
C CIRCULAR LOOP ANTENNA. THE CURRENT IS CALCULATED AS A FUNCTION OF PHI AT
C 10 INSTANTS OF TIME. THE LOOP IS DRIVEN AT PHI=0. THE WIRE RADIUS =A, THE
C LOOP RADIUS=R.
C SUBROUTINES OR SUBFUNCTIONS TO BE USED WITH THIS PROGRAM ARE
C     SUBROUTINE BETAN
C     SUBROUTINE RR
C     SUBROUTINE SICINT
C     SUBFUNCTION E
DIMENSION T(10),BE(10,30),BET(199,30),TA(6),TB(6),TC(6)
DIMENSION G(100)
COMMON/A/CUR( 301),PHI(1751),K(31),BETA(30),R(1025)
COMMON/R/AOR,BK,GAMMA1,JKB,AOROL
TYPE COMPLEX J,JKB,K, BETA,EW,E
DATA PI,C,J/3.1415927,3.58,(0.,1.)/
C THESE VALUES OF A AND B ARE SUCH THAT OMEGA=2*ALOG(2*PI*B/A)=10. OTHER VALUES
C OF OMEGA CAN BE USED BY CHANGING A OR B OR BOTH.
A=4.23357E-2
R=1.
AOR=(A/B)**2
COB=C/R
AOROL=-1.
ERR=1.E-3
T(1)=PI*0.25
DTI=T(1)*0.1
DO 4 I=2,10
4 T(I)=T(I-1)+PI*0.25
CON=2.*C/(PI*PI*120.*PI*R)
DO 6 IA=1,10
DO 6 IB=1,30
6 RE(IA,IB)=0.
EX=EXP(1.)
DEL=3./(EX*EX)
IZ=6
IY=IZ+1
IYO=IY
W=1.E-3
BK=W/COR
JKB=J*BK
CALL BETAN(30,ERR)
EW=E(COB*BK,2)/JKB
BET(IYO,1)=REAL(EW*BETA(1)*JKB*COR)
DO 17 I=2,30
17 BET(IYO,I)=REAL(EW*BETA(I))
DO 3 IB=1,18
DO 16 I=1,30
16 BET(1,I)=BET(IYO,I)
DEL=DEL*EX
DBK=DEL/(COB*IZ)
BKL=BK
IF(IB.NF.18) GO TO 18
BKU=10.
IZ=198
DBK=(BKU-BKL)/IZ

```

```

      IY=IZ+1
13 DO 1 I=2,IY
      BK=BK+DBK
      JKB=J*BK
      CALL BETAN(30,ERR)
      EW=E(COR*BK,2)/JKB
      BET(I,1)=REAL(EW*BETA(1)*J*BK*COB)
      DO 2 IA=2,30
2 BET(I,IA)=REAL(EW*BETA(IA))
1 CONTINUE
      BKB=BK
      DO 5 IA=1,30,2
      DO 5 IC=1,10
      CALL SICOINT(BKL,BKU,IZ,T(IC),BET(1,IA),BET(1,IA+1),UA,UZ,UB,UY)
      IF(IA.EQ.1) GO TO 13
      BE(IC,IA)=BE(IC,IA)+CON*UA
13 BE(IC,IA+1)=BE(IC,IA+1)+CON*UB
5 CONTINUE
      TI=DTI
      DO 14 I=1,100
      CALL SICOINT(BKL,BKU,IZ,TI,BET(1,1),BET(1,2),G(I),UZ,UB,UY)
14 TI=TI+DTI
      DO 15 I=2,100
      G(1)=G(1)+G(I)
      IF(MOD(I,10).NE.0) GO TO 15
      ISUB=I/10
      BE(ISUB,1)=BE(ISUB,1)+(G(1)-0.5*G(I))*CON*DTI/COB
15 CONTINUE
3 CONTINUE
      DP=PI/150.
C PHI(I) I=1,2,...,301 ARE THE ANGLES AT WHICH THE CURRENT DISTRIBUTION IS
C CALCULATED.
      PHI(1)=-PI
      DO 7 I=2,301
7 PHI(I)=PHI(I-1)+DP
      DO 8 I=1,10
      DO 9 IA=1,301
11 FORMAT(10E13.4)
      CUR(IA)=BE(I,1)
      DO 9 IB=2,30
9 CUR(IA)=CUR(IA)+BE(I,IB)*COS((IB-1)*PHI(IA))
C T(I)=I*PI/4=TIME*(VELOCITY OF LIGHT)/B, I=1,2,...,10.
      PRINT 11,T(I)
      PRINT 12
C CUR(J)=THE VALUE OF THE TRANSIENT CURRENT AT PHI(J) AND AT T(I).
      PRINT 11,CUR
      PRINT 12
      IY=301*(I-1)
      DO 10 IA=1,301
      IZ=IY+IA
10 BET(IZ)=CUR(IA)
8 CONTINUE
      PRINT 11,BE
C BE(I,J) ARE THE FOURIER COEFFICIENTS AT T(I).
12 FORMAT(////////)
      END

```

```

PROGRAM PATTERN(INPUT,OUTPUT,TAPE10)
C THIS PROGRAM COMPUTES THE FIELD PATTERNS OF A CIRCULAR LOOP ANTENNA.
C SUBROUTINES OR SUBFUNCTIONS TO BE USED WITH THIS PROGRAM ARE
C     SUBROUTINE RETAN
C     SUBROUTINE RR
C     SUBROUTINE PICK
DIMENSION X(101),Y(101),ANGLE(101),TA(6),TR(6)
DIMENSION U(107,19,5),V(107,19,5),Z(101)
COMMON/A/EFG(3199)
COMMON/R/AOR,RK,GAMM1,JKB,AOBOL
COMMON/C/THETA,PHI,CON,M,ERR,ETHETA,EPhi,AOBO,DBKO,ERROR
TYPE COMPLEX J,JKB,ETHETA,EPhi
DATA PI,C,J/3.1415927,3.E8,(0.,1.)/
CALL HDCOPY(10)
CALL ENTFLN(10)
CON=-0.25/(PI*PI)
C THE WIRE RADIUS=A, THE LOOP RADIUS=B, BOTH IN METERS.
C R IS THE DISTANCE FROM THE LOOP TO THE OBSERVER.
C THESE VALUES OF A AND B ARE SUCH THAT OMEGA=2*ALOG(2*PI*B/A)=10. OTHER VALUES
C OF OMEGA CAN BE USED BY CHANGING A OR B OR BOTH.
R=1.E4
CON=CON/R
A=4.23357E-2
B=1.
AOB=(A/B)**2
AOBOL=-1.
AOPO=-1.
DBKO=-1.
ERROR=0.
ERR=1.E-3
DA=PI/50.
RK=1.
DBK=0.5
ANGLE(1)=-PI/2.
DO 1 I=2,101
1 ANGLE(I)=ANGLE(I-1)+DA
DO 20 I=1,5
DO 20 IA=1,19
DO 20 IB=102,107
U(IB,IA,I)=0.
20 V(IB,IA,I)=0.
DO 2 I=1,19
PRINT 6
PRINT 5,A,B,BK
C A=THE WIRE RADIUS, B=THE LOOP RADIUS, BOTH IN METERS. BK=B*2*PI*FREQUENCY/(
C THE VELOCITY OF LIGHT).
PRINT 6
M=3.*BK
IF(M.LT.5) M=5
JKB=J*BK
C FROM HERE TO STATEMENT NUMBER 9 THE PATTERN IN THE THETA=PI/2 PLANE IS
C CALCULATED.
THETA=PI*0.5
DO 3 IA=26,76
PHI=ANGLE(IA)

```

```

CALL FAR E
IZ=IA-25
3 X(IZ)=CABS(EPHI)
CALL PICK(X,51,XMAX)
PRINT 5,XMAX
DO 9 IA=26,76
PHI=ANGLE(IA)
IZ=IA-25
U(IZ,I,1)=X(IZ)*COS(PHI)/XMAX
V(IZ,I,1)=X(IZ)*SIN(PHI)/XMAX
U(102-IZ,I,1)=U(IZ,I,1)
9 V(102-IZ,I,1)=-V(IZ,I,1)
C FROM HERE TO STATEMENT NUMBER 8 THE PATTERN IN THE PHI=0 PLANE IS CALCULATED.
PHI=0.
DO 7 IA=1,51
THETA=ANGLE(IA)
CALL FAR E
7 X(IA)=CABS(EPHI)
CALL PICK(X,51,XMAX)
PRINT 5,XMAX
DO 3 IA=1,51
THETA=ANGLE(IA)
U(IA,I,2)=X(IA)*SIN(THETA)/XMAX
V(IA,I,2)=X(IA)*COS(THETA)/XMAX
IZ=102-IA
U(IZ,I,2)=U(IA,I,2)
8 V(IZ,I,2)=-V(IA,I,2)
C FROM HERE TO STATEMENT NUMBER 2 THE PATTERNS IN THE PHI=PI/2 PLANE ARE
C CALCULATED.
PHI=PI/2.
DO 11 IA=1,26
THETA=ANGLE(IA)
CALL FAR E
X(IA)=CABS(EPHI)
Y(IA)=CABS(ETHETA)
11 Z(IA)=SQRT(X(IA)**2+Y(IA)**2)
CALL PICK(X,26,XMAX)
CALL PICK(Y,26,YMAX)
CALL PICK(Z,26,ZMAX)
PRINT 5,XMAX,YMAX,ZMAX
DO 12 IA=1,26
ST=SIN(ANGLE(IA))
CT=COS(ANGLE(IA))
U(IA,I,3)=X(IA)*ST/XMAX
V(IA,I,3)=X(IA)*CT/XMAX
U(IA,I,4)=Y(IA)*ST/YMAX
V(IA,I,4)=Y(IA)*CT/YMAX
U(IA,I,5)=Z(IA)*ST/ZMAX
V(IA,I,5)=Z(IA)*CT/ZMAX
IZ=52-IA
U(IZ,I,3)=-U(IA,I,3)
U(IZ,I,4)=-U(IA,I,4)
U(IZ,I,5)=-U(IA,I,5)
V(IZ,I,3)=V(IA,I,3)
V(IZ,I,4)=V(IA,I,4)

```



```

12 V(IZ,I,5)=V(IA,I,5)
   DO 13 IA=1,51
      IZ=102-IA
      DO 13 IR=3,5
         U(IZ,I,IR)=U(IA,I,IR)
13 V(IZ,I,IR)=-V(IA,I,IR)
C THE REMAINING PORTION OF THE PROGRAM IS USED FOR PLOTTING ONLY.
2 BK=BK+DBK
   DO 17 IC=1,5
      DO 14 I=1,20,4
         YY=11.-2.5*((I+4)/4-1)
         DO 15 IA=1,4
            IZ=I+IA-1
            IF(IZ.EQ.20) GO TO 15
            XX=2.25+2.5*(IA-1)
            DO 18 ID=1,3
               U(ID+101,IZ,IC)=XX+ID-2.
               V(ID+101,IZ,IC)=YY
               U(ID+104,IZ,IC)=XX
10 V(104+ID,IZ,IC)=YY+ID-2.
            DO 16 IR=1,101
               U(IR,IZ,IC)=U(IR,IZ,IC)+XX
16 V(IR,IZ,IC)=V(IR,IZ,IC)+YY
15 CONTINUE
14 CONTINUE
17 CONTINUE
   DO 19 IC=1,5
      U(105,2,IC)=12.
19 V(106,2,IC)=12.
      NPS=107*19
      DO 21 I=1,5
         CALL GRID1V(4,0.,12.,0.,12.,0,0,0,0,-0,-0,0,0,3,3)
         CALL APL0TV(NPS,U(1,1,I),V(1,1,I),1,1,1,42,IEPP)
21 CONTINUE
4 FORMAT(6A10)
5 FORMAT(10E13.4)
6 FORMAT(////////)
CALL EXTFLM(0)
END

```

```

SUBROUTINE VOCZA(VOC,ZA)
C THIS SUBROUTINE CALCULATES THE OPEN CIRCUIT VOLTAGE TRANSFER FUNCTION AND THE
C ANTENNA IMPEDENCE FOR A LOOP ANTENNA.
COMMON/A/INTG(1026),K(31),BETA(30),R(1025)
COMMON/R/AOB,BK,GAMMA1,JBK,AOBOL,ERRB
COMMON/C/EX,EY,EZ,L,M,N,B,FRR,ER,NCALL
TYPE COMPLEX INTG,K,BETA,JBK,INT,INTO,ZA,VOC
TYPE REAL L,M,N
DIMENSION ST(257)
DATA PI/3.1415927/
IF(NCALL.FO.1) GO TO 1
NCALL=1
DTHETA=PI/512.
THETA=0.
ST(1)=0.
DO 2 I=2,257
THETA=THETA+DTHETA
2 ST(I)=SIN(THETA)
1 JBK=CMPLX(0.,BK)
NQ=3.*BK
IF(NQ.LT.5) NQ=5
CALL BETAN(NQ,ERR)
ZA=BETA(1)
DO 3 I=2,NQ
3 ZA=ZA+BETA(I)
J=0
INTO=(0.,0.)
VOC=INTO
DO 7 IB=1,NQ
DTHETA=PI/16.
DTHETA2=DTHETA
AI=IB-1
THETA=0.
MM=1
MN=32
DO 4 I=1,6
IF(J.GE.I) GO TO 6
J=I
DO 5 IA=MM,256,MN
JA=258-IA
INTG(IA)=CMPLX(EY*ST(JA)-EX*ST(IA),0.)*CEXP(CMPLX(0.,-BK*(L*ST(JA)
1+M*ST(IA))))
JB=256+IA
INTG(JB)=CMPLX(-EY*ST(IA)-EX*ST(JA),0.)*CEXP(CMPLX(0.,-BK*(-L*ST(I
1A)+M*ST(JA))))
JB=JB+256
INTG(JB)=CMPLX(EX*ST(IA)-EY*ST(JA),0.)*CEXP(CMPLX(0.,+BK*(L*ST(JA)
1+M*ST(IA))))
JB=JB+256
5 INTG(JB)=CMPLX(EX*ST(JA)+EY*ST(IA),0.)*CEXP(CMPLX(0.,-BK*(L*ST(IA)
1-M*ST(JA))))
6 INT=(0.,0.)
DO 8 IA=MM,1024,MN
INT=INT+INTG(IA)*COS(AI*THETA)
8 THETA=THETA+DTHETA2

```

```

INT=INT*DTHETA+INTO*CMPLX(0.5,0.)
ER=CABS(INT-INTO)/CABS(INT)
INTO=INT
IF(ER.LT.FRR) GO TO 9
DTHETA2=DTHETA
DTHETA=0.5*DTHETA
MM=1+2**(5-I)
MN=2**(6-I)
4 THETA=DTHETA
9 VOC=VOC+BETA(IR)*INT
7 CONTINUE
ZA=(1.,0.)/ZA
VOC=B*ZA*VOC*CEXP(CMPLX(0.,-BK*SQRT(1.-N*N)))
ZA=ZA*CMPLX(0.,PI*PI*BK*120.)
RETURN
END

```

```

SUBROUTINE BETAN(M,FRR)
C THIS SUBROUTINE CALCULATES THE FOURIER COEFFICIENTS FOR THE TRANSMITTING
C CURRENT DISTRIBUTION ON A LOOP WHEN DRIVEN BY THE VOLTAGE V=CEXP(+JWT).
C BETA(I),I=1,2,...,M, IS RETURNED THROUGH COMMON/A/.
COMMON/A/E(1025),K(31),BETA(30),R(1025)
COMMON/R/AOB,BK,GAMMA1,JKR,AOSOL,ERRB
TYPE COMPLEX JKR,E,S,SN,K,BETA
DATA PI/3.1415927/
CALL RR(1,32)
M1=M+1
L=1
DO 1 I=1,M1
AA=I-1
H=PI/32.
SN=0.
X=H
S=0.5*H*(E(1)+E(1025)*COS(AA*PI))
DO 2 J=33,1024,32
SN=SN+E(J)*COS(X*AA)
2 X=X+H
S=SN*H +S
DO 3 J=1,5
MM=1+2*(5-J)
MN=2*(6-J)
IF(J.LT.L) GO TO 4
L=L+1
CALL RR(MM,MN)
4 H2=H
H=0.5*H
X=H
SN=0.
DO 5 JJ=MM,1024,MN
SN=SN+E(JJ)*COS(X*AA)
5 X=X+H2
SN=SN*H+S*0.5
IF(CABS(SN).EQ.0.) GO TO 6
C=CABS((SN-S)/SN)
GO TO 7
6 C=CABS(SN-S)
7 IF(C.LT.ERR) GO TO 8
3 S=SN
IF(C.GT.ERRB) ERRB=C
8 K(I)=SN/PI
1 CONTINUE
BETA(1)=1./K(2)
DO 10 I=2,M
L=I-1
10 BETA(I)=4./(K(I+1)+K(L)-2.*(L/BK)**2*K(I))
RETURN
END

```

```

SUBROUTINE RR(M,N)
C THIS SUBROUTINE IS CALLED FROM SUBROUTINE BETAN ONLY. R(I),I=1,2,...,1025, IS
C RETURNED THROUGH COMMON/A/.
COMMON/A/E(1026),K(31),BETA(30),R(1025)
COMMON/R/AOB,BK,GAMMA1,JKB,AOBOL,ERRB
TYPE COMPLEX JKB,E,K,BETA
IF(AOB.NE.AOBOL) GO TO 1
4 DO 2 I=M,1025,N
2 E(I)=CEXP(-JKB*R(I))/R(I)
RETURN
1 DX=3.1415927/1024.
X=DX.
S4=0.
S2=0.
DO 3 I=2,1024,2
CX=COS(X)
R(I)=SQRT(AOB+2.*(1.-CX))
S4=S4+CX/R(I)
X=X+DX
CX=COS(X)
R(I+1)=SQRT(AOB+2.*(1.-CX))
S2=S2+CX/R(I+1)
3 X=X+DX
R(1)=SQRT(AOB)
R(1025)=SQRT(AOB+4.)
GAMMA1=(1./R(1)-1./R(1025)+4.*S4+2.*S2)*DX/3.
GAMMA1=1./GAMMA1
AOBOL=AOB
GO TO 4
END

```

```

SUBROUTINE FAR F
C THIS SUBROUTINE COMPUTES THE FAR FIELD COMPONENTS OF THE ELECTRIC FIELD FROM A
C LOOP WHICH IS DRIVEN BY THE VOLTAGE V=CEXP(+JWT). THE COMPONENTS ARE IN THE
C THETA AND PHI DIRECTIONS. THE LOOP IS IN THE X-Y PLANE AT Z=0. ETHETA AND
C EPHI ARE RETURNED THROUGH COMMON/C/.

```

```

COMMON/A/SE(513),CE(513),K(31),BETA(30),R(1025)
COMMON/R/AOB,BK,GAMMA1,JKB,AOBOL,ERRB
COMMON/C/THETA,PHI,CON,M,ERR,ETHETA,EPHI,AOBO,BKO,ERROR
TYPE COMPLEX JKB,SE,CE,ETHETA,EPHI,ST,E,ETO,EPO,ETHET,EPH,K,BETA
DATA PI/3,1415927/
IF(AOB.EQ.AOBO.AND.BK.EQ.BKO) GO TO 14
AOBO=AOB
BKO=BK
CALL RETAN(M,ERR)
14 ST=SIN(THETA)*JKB
ANGLE=PHI+PI
DA=PI/16.
DO 1 I=1,513,16
CA=COS(ANGLE)
E=CEXP(ST*CA)
CE(I)=CA*E
SE(I)=E*SIN(ANGLE)
1 ANGLE=ANGLE-DA
L=1
ETHETA=0.
EPHI=0.
DO 2 I=1,M
AA=I-1
ETHET=0.
EPH =0.
DA=PI/16.
ANGLE=-PI+DA
CA=COS(PI*AA)
ETO=0.5*DA*(SE(1)+SE(513))*CA
EPO=0.5*DA*(CE(1)+CE(513))*CA
DO 3 J=17,512,16
CA=COS(ANGLE*AA)
ETHET =ETHET+SE(J)*CA
EPH =EPH +CE(J)*CA
3 ANGLE=ANGLE+DA
ETO=ETO+ETHET *DA
EPO=EPO+EPH *DA
DO 4 J=1,4
MM=1+2**(4-J)
MN=2**(5-J)
DA2=DA
DA=0.5*DA
ETHET =0.
EPH =0.
IF(J.LT.L) GO TO 5
L=L+1
ANGLE=PHI+PI-DA
DO 6 JJ=MM,512,MN
CA=COS(ANGLE)
E=CEXP(ST*CA)

```

```

CE(JJ)=E*CA
SE(JJ)=E*SIN(ANGLE)
6 ANGLE=ANGLF-DA2
5 ANGLF=-PI+DA
DO 7 JJ=MM,512,MN
CA=COS(ANGLE*AA)
ETHET =ETHET +SE(JJ)*CA
EPH =EPH +CE(JJ)*CA
7 ANGLE=ANGLE+DA2
ETHET =ETHET*DA+ETO*0.5
EPH =EPH*DA+EPO*0.5
ETM=CABS(ETHET)
EPM=CABS(EPH )
IF(ETM.GT.EPM) GO TO 8
ETM=CABS(EPH -EPO)
GO TO 9
8 EPM=ETM
ETM=CABS(ETHET -ETO)
9 IF(EPM.EQ.0.) GO TO 10
EPM=ETM/EPM
GO TO 11
10 EPM=ETM
11 IF(EPM.LT.ERR) GO TO 12
ETO=ETHET
4 EPO=EPH
IF(EPM.GT.ERROR) ERROR=EPM
12 ETHETA=ETHETA+ETHET*BETA(I)
2 EPHI=EPHI+EPH*BETA(I)
ETHETA=ETHETA*COS(THETA)*CON
EPHI=ERHI*CON
RETURN
END

```

```

SUBROUTINE SICOINT(L,U,N,W,F1,F2,F1CO,F1SI,F2CO,F2SI)
C   INTEGRATION OF F1(X)*COS(WX), F1(X)*SIN(WX), F2(X)*COS(WX), AND
C   F2(X)*SIN(WX), WHERE (L,U) IS THE RANGE OF INTEGRATION,
C   AND N IS THE NUMBER OF MESH INTERVALS TAKEN. THEREFORE,
C   IT IS REQUIRED THAT THE FUNCTION ARRAYS F1, AND F2
C   EACH HAVE N+1 POINTS. N MUST BE AN EVEN INTEGER.
C   W MAY BE ZERO OR A POSITIVE OR NEGATIVE REAL NUMBER.
C   THE FUNCTION ARRAYS F1, AND F2 AND THE COMPUTED
C   INTEGRALS F1CO, F1SI, F2CO, F2SI ARE REAL VARIABLES.
C   METHOD--THE FUNCTIONAL VALUES OF THE F-ARRAYS ARE FITTED
C   BY SUCCESSIVE MOVING ARC PARABOLAS, AND THE RESULTING
C   POLYNOMIAL*SINUSOIDAL EXPRESSIONS ARE EVALUATED IN CLOSE FORM.
C   BY COMPUTING BASIC COEFFICIENTS DURING THE INITIAL PHASE THESE
C   CALCULATIONS REDUCE TO SUMMATIONS WITH CONCURRENT EVALUATION
C   OF TRIGONOMETPIC FACTORS BY RECURRENCE RELATIONS.
C   DOUBLE PRECISION ARITHMETIC IS USED FOR CERTAIN
C   CALCULATIONS TO PREVENT LOSS OF SIGNIFICANCE.
C   ALPHONSE IACOLETTI
C   ORG. 9422, SANDIA CORPORATION
C   MARCH, 1966
      DIMENSION F1(1),F2(1)
      TYPE INTEGER N
      TYPE REAL L,U,LAM2,LAM1,LAM0,MU2,MU0
      TYPE DOUBLE DL,DU,DH,DW,DWH,DWWH,DCWH,DSWH,DDEL1,
1DCWX,DSWX,DC2WH,DS2WH,D1,D2,D3,D4
      TYPE DOUBLE DHOV3,F1SUM1,F1SUM2,F2SUM1,F2SUM2,C1,S1,C2,S2
1000 IF(N)1100,1101,1020
1020 IF(N-2*(N/2))1100,1040,1100
1040 C1=0.D
      S1=0.D
      C2=0.D
      S2=0.D
      NMI1=N-1
      DL=L
      DU=U
      DH=(DU-DL)/N
1060 IF(DH)1080,1900,1080
1080 IF(W)1200,2000,1200
1100 PRINT 1110,L,U,N,W
1110 FORMAT(38H0ERROR DETECTED IN SUBROUTINE SICOINT.
      137H THE ARGUMENTS L, U, N, AND W ARE ---/
      21X,2E20.10,I16,E20.10)
      STOP
1200 DW=W
      DWH=DH*DW
      DWWH=DWH*DW
      DCWH=DCOS(DWH)
      DSWH=DSIN(DWH)
      D1=DSWH/DWH
      DDEL1=(2.D/DWWH)*(DCWH-D1)
      LAM1=-2.D*DDEL1
      LAM2=DDEL1+DSWH/DW
      LAM0=LAM2
      MU2=(D1-DCWH)/DW
      MU0=-MU2

```



```

D2=DW*(DL+DH)
DCWX=DCOS(D2)
DSWX=DSIN(D2)
D3=2.D*DWH
DC2WH=DCOS(D3)
DS2WH=DSIN(D3)
1500 DO 1800 I=1,NMI,2
    CWX=DCWX
    SWX=DSWX
1600 F1I=F1(I)
    F1IP1=F1(I+1)
    F1IP2=F1(I+2)
    R1=LAM2*F1IP2+LAM1*F1IP1+LAM0*F1I
    R2=MU2*F1IP2+MU0*F1I
    C1=C1+(R1*CWX-R2*SWX)
    S1=S1+(R1*SWX+R2*CWX)
1700 F2I=F2(I)
    F2IP1=F2(I+1)
    F2IP2=F2(I+2)
    R3=LAM2*F2IP2+LAM1*F2IP1+LAM0*F2I
    R4=MU2*F2IP2+MU0*F2I
    C2=C2+(R3*CWX-R4*SWX)
    S2=S2+(R3*SWX+R4*CWX)
    D4=DCWX*DC2WH-DSWX*DS2WH
    DSWX=DSWX*DC2WH+DCWX*DS2WH
    DCWX=D4
1800 CONTINUE
1900 F1CO=C1
    F1SI=S1
    F2CO=C2
    F2SI=S2
    RETURN
2000 DHOV3=DH/3.D
    F1SUM1=0.D
    F1SUM2=0.D
    F2SUM1=0.D
    F2SUM2=0.D
2100 DO 2200 I=2,N,2
    F1SUM1=F1SUM1+F1(I)
    F1SUM2=F1SUM2+F1(I+1)
    F2SUM1=F2SUM1+F2(I)
    F2SUM2=F2SUM2+F2(I+1)
2200 CONTINUE
2300 C1=DHOV3*(F1(1)+(4.D*F1SUM1+(2.D*F1SUM2-F1(N+1))))
    C2=DHOV3*(F2(1)+(4.D*F2SUM1+(2.D*F2SUM2-F2(N+1))))
    GO TO 1900
3000 RETURN
1101 F1CO=F1SI=F2CO=F2SI=0.
    RETURN
    END

```

```
FUNCTION F(W,I)
C THIS SUBFUNCTION IS AN EXAMPLE OF THE FOURIER TRANSFORM OF THE TRANSIENT DRIVE
C VOLTAGE.
```

```
COMPLEX E
DATA A/1.3333333E-9/
GO TO (1,2),I
1 E=(1.,0.)/CMPLX(1.,W)
RETURN
2 E=(1.,0.)/(CMPLX(1.,W)*CMPLX(1.,W*A)**2)
RETURN
END
```

```
FUNCTION ZL(W,I)
C THIS FUNCTION SUBPROGRAM IS AN EXAMPLE OF A LOAD IMPEDENCE FUNCTION.
```

```
COMPLEX ZL
GO TO (1,2,3,4,5,6,7,8),I
1 ZL=CMPLX(1.E50,0.)
RETURN
2 ZL=CMPLX(5000.,0.)
RETURN
3 ZL=CMPLX(1000.,0.)
RETURN
4 ZL=CMPLX( 500.,0.)
RETURN
5 ZL=CMPLX( 250.,0.)
RETURN
6 ZL=CMPLX(  50.,0.)
RETURN
7 ZL=CMPLX(   1.,0.)
RETURN
8 ZL=CMPLX(  0.5,0.)
RETURN
END
```

```
SUBROUTINE PIC(F,N,FMAX,FMIN)
DIMENSION F(1)
FMAX=F(1)
FMIN=F(1)
DO 1I=2,N
IF(F(I).GT.FMAX) FMAX=F(I)
IF(F(I).LT.FMIN) FMIN=F(I)
1 CONTINUE
RETURN
END
```